Pattullo Bridge Project

Underwater Acoustic Modelling for Pile Driving Operations

Submitted to:

Andrew Duthie
Hatfield Consultants
#200–850 Harbourside Drive
North Vancouver, BC V7P 0A3
Tel: +1-604-926-3261

Authors:

Mikhail Zykov
Cynthia Pyć
Alex McGillvray

1 March 2018

JASCO Applied Sciences (Canada) Ltd
Suite 2305, 4464 Markham St.
Victoria, BC V8Z 7X8 Canada
Tel: +1-250-483-3300
Fax: +1-250-483-3301
www.jasco.com

P001402-002
Document 01530
Version 2.2

Document Version Control

Version	Date	Name	Change
0.1	2017 Nov 27	C Pyć	Initial Draft
0.2	2017 Nov 27	A McGillvray	Draft review and additions
1.0	2017 Dec 7	C Pyć	Draft released to client for review
1.1	2017 Dec 11	C Pyć	Addressing client comments
1.2	2017 Dec 12	C Pyć	Final report released to client
1.3	2018 Jan 15	C Pyć	Amended report to include mitigation of modeled scenarios
2.0	2018 Jan 24	C. Pyć	New Scope of Work includes additional scenarios and mitigation
2.0	2018 Jan 25	C. Pyć	Amended Draft report released to client
2.1	2018 Feb 26	C. Pyć	New Scope of Work added to report and released to client
2.2	2018 Mar 1	C. Pyć	Amended Draft report released to client

Suggested citation:

Zykov, M., C. D. Pyć., and A. McGillvray. 2017. *Pattullo Bridge Project:* Underwater Acoustic Modelling for Pile Driving Operations. Document 01530, Version 2.2. Technical report prepared by JASCO Applied Sciences for Hatfield Consultants.

Executive Summary

The Pattullo Bridge Replacement Project ("Project") involves the construction of a four-lane bridge across the Fraser River. The new bridge connects the cities of Surrey and New Westminster, British Columbia, north and upstream of an existing bridge that will be decommissioned upon completion of the new crossing. The Project involves the installation of multiple piers with four in-river pier supports. Project model assumptions include the following: in-river piers require approximately sixty-two (62) hammer-driven and drilled piles; the footing of the piles is planned to reach a depth of 50 m below the sediment surface; and concurrent pile driving may take place with multiple piles driven at the same time at different sites. Construction is anticipated to commence in third quarter 2019, with pile-driving activity scheduled over a 10 month period.

This report by JASCO Applied Sciences (JASCO) presents the results of acoustic modelling of underwater noise generated during piling installation. Pile driving noise is transmitted from the pipe pile through river sediments and sheet pile wall, and into the water. Acoustic models predict the sound levels and ranges to acoustic thresholds in water that may result in injury to valued ecosystem components (VCs) such as fish (e.g. sturgeon and Pacific salmon). The basic modelling approach is to characterize the sound source and then determine how the sounds propagate in the specific construction areas. The modelling results inform the environmental impact assessment of the potential effects of pile driving on VCs that may be present in the vicinity of the Project during construction.

JASCO has determined from similar studies that impact hammer installation of piles results in the highest noise levels. In this study, a conservative modelling assumption approach was adopted because of the Project's early planning stage and operational uncertainty. The worst-case likely scenario involves a maximum four (4) - 1800 mm steel piles hammer-installed to 50 metres simultaneously at all the proposed pier locations. Mitigation measures implemented during pile driving can decrease the potential impacts to fish by reducing the zone of potential impact and therefore the likelihood of injurious sound interaction. Mitigation under consideration includes double-walled steel piles, cofferdams and/or confined bubble curtains. Various studies have demonstrated that these mitigation measures are capable of attenuating sounds by approximately 10 dB to 23 dB (Reinhall et al. 2015, Christopherson and Lundberg 2013, Bellman 2014).

Acoustic thresholds used in this study represent the best available science available on the effects of sound on fish, from Popper et al. 2014. The Guidelines established by Popper et al. (2014) represent the consensus efforts of a scientific working group to establish sound exposure guidelines for fishes and fish eggs and larvae, across the complete range of taxa and sound types, considering mortality and injury.

The results of the analysis, using a worst case scenario of four piles simultaneously installed at all four pier locations, indicate that the unmitigated maximum range to Sound Exposure Level (SEL) acoustic thresholds over a 24-hour period for fish with swim bladders not involved in hearing is approximately 176 metres, or 201 metres peak Sound Pressure Level (peak SPL) for mortality and potential mortal injury. The affected area for recoverable injury based on these SEL thresholds over 24-hours, for fish with swim bladders (e.g. salmonids and sturgeon), is approximately 328 m^2. Analysis of mitigated sound levels, based on test measurements of double-walled piles conducted in Puget Sound, Washington, (assuming a 13.8–17.2 dB SEL and 12–21.2 dB peak SPL reduction), result in substantially decreased ranges for mortality and potential mortal injury. For example, 176 metres (SEL) and 201 metres (peak SPL) are reduced to ranges very near to the impact pile driving sound source: 7-11 metres and 4-24 metres respectively when mitigation is applied to the acoustic model, and the affected area for recoverable injury is reduced to 3.4-9.5 m^2. These model predictions assume that the biological receiver (e.g., fish) is stationary for the duration of the sound exposure. Sound reduction and related ensonified ranges will vary with different mitigation measures.

Project pile driving sounds are predicted to attenuate to background levels over several kilometres assuming an unobstructed straight line. River bends, islands and in-river infrastructure will increase the attenuation of sound, therefore modelled ranges to sound levels that could potentially elicit behavioural response are considered conservative. Fish with swim bladders not involved in hearing, which include sturgeon and Pacific salmon, are predicted to be at moderate risk of behavioural response at intermediate distances (10s of meters from the source) and low risk at greater distances, even when piling source

sound levels exceed background noise levels. Eggs and larvae are predicted to be at lower risk than adults for behavioural response. Behavioural response of fish to impulsive sounds including pile driving is highly variable, including no response, startle response, avoidance, and habituation.

Contents

Figures

Tables

1. Introduction

The Pattullo Bridge Replacement Project ("Project") involves the construction of a four-lane bridge across the Fraser River. The new bridge connects the cities of Surrey and New Westminster, British Columbia, north and upstream of an existing bridge that will be decommissioned upon completion of the new crossing. The modelled Project involves the installation of multiple piers with four placed in the river (Figure 1). The four in-river pier supports are comprised of approximately sixty-two (62) hammer-driven and drilled piles. The footing of the piles is planned to reach a depth of 50 m below the sediment surface. Concurrent pile driving may take place with multiple piles driven at the same time at different sites. Up to four (4) simultaneous piles were modeled to calculate the cumulative sound footprint of this activity level.

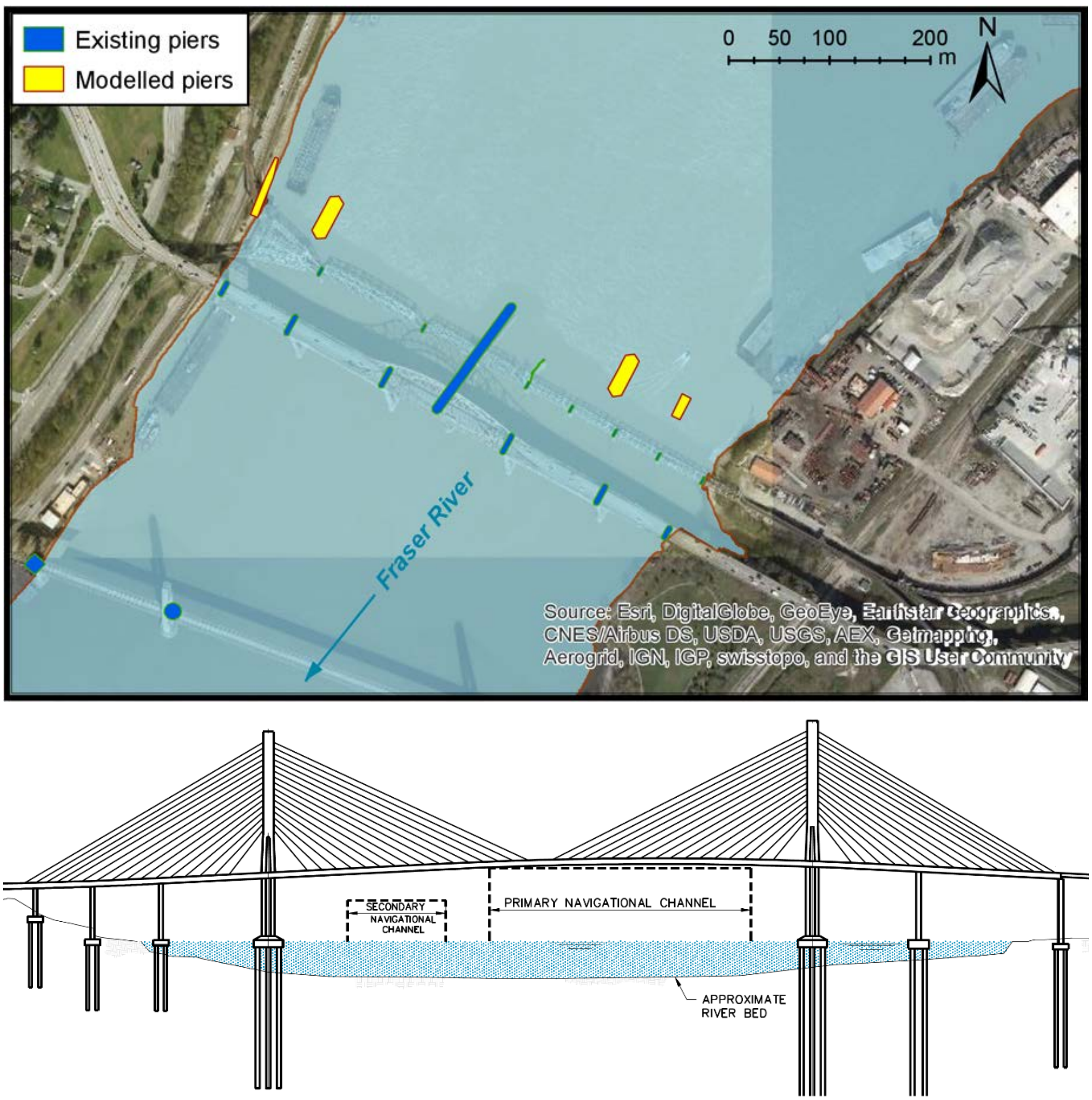

Figure 1. Overview of the planned construction area with indicated footprint of (top) the modelled piers and (bottom) bridge schematics. Image provided by Hatfield Consultants 2017.

This report by JASCO Applied Sciences (JASCO) presents the results of acoustic modelling of underwater sound generated during piling installation. The sound is transmitted from the pipe pile through river sediments and sheet pile wall, and into the water. Acoustic models predict the sound levels and ranges to acoustic thresholds in water that may result in injury to valued components (VCs) such as fish (e.g., sturgeon and Pacific salmon). The basic modelling approach is to characterize the unmitigated and mitigated sound source and then determine how the sounds propagate in a specific construction area. The modelling results inform the assessment of potential effects of pile driving on VCs that may be present in the vicinity of the Project during construction.

1.1. Piling Installation as a Sound Source

For most projects involving pile driving in shallow-water environments, there is a potential for direct transmission from the source to biological receivers such as fish, and there are reflected paths from the surface and the bottom that may be perceived by fish and other fauna. Normally the ground-radiated sound is dominated by low frequencies that cannot propagate efficiently through shallow water. When impulsive pile driving is the sound source, there is the potential for substrate-borne sound that results from the pile being struck by the hammer, which is then re-radiated back into the water where it may reach a biological receiver. Energy transmission through water depends on the following factors for pile driving: 1) direct contact of the pile and water; 2) the depth of the water column; 3) the size of the pile; 4) type of hammer; and 5) the energy of the hammer (Christopherson and Lundberg 2013). Obstructions, such as barges, other piles and structures (e.g., existing bridges), and river channel characteristics, such as the narrowness of the channel and the slope of channel sides, can modify how sound propagates in water (Buehler et al. 2015). Figure 2 illustrates these basic propagation concepts.

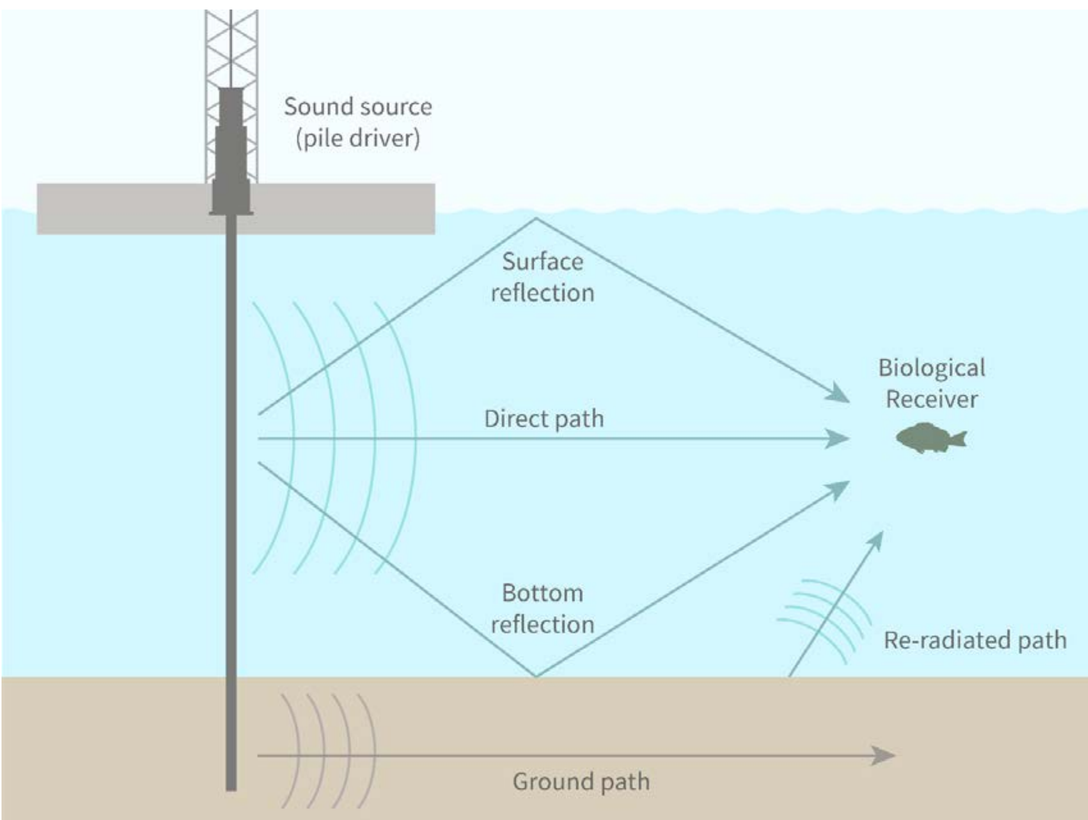

Figure 2. Underwater sound propagation paths associated with pile driving (adapted from Buehler et al. 2015).

1.2. Modelling Scope & Assumptions

Sound generated during pile driving varies with the energy required to install the piles to the desired depth, which depends on the sediment resistance encountered. Sediment types with greater resistance require pile drivers that deliver higher energy strikes. The maximum noise levels from pile driving usually occur at the last stage (Betke 2008). A pile is a distributed sound source because its entire length excites pressure waves in the water. For modelling purposes, the pile is represented by a vertical array of point sources, distributed over the water column and into the seabed. Because the specifications for the impact hammer were not provided at the time of modelling, literature data was used to estimate source levels for pile driving and to select a hammer type appropriate for the proposed pile sizes.

This report assesses the use of impact hammering for pile installation. It is assumed that all piling locations will utilize 1800 mm pre-fabricated steel driven piles hammered to a total depth of 50 m using a piling rig. From previous project modelling, JASCO has determined that impact hammer installation of piles can result in high sound levels. In this modelling study, a conservative approach was taken by assuming hammer installation for all in-river pile locations, with a simultaneous pile installation scenario. A worst-case likely scenario involves a maximum four (4) piles installed simultaneously at all pier locations. Additional modelling assumptions include:

- 1800 mm steel cylindrical pilings with wall thickness of 32 mm.
- total installation depth: 50 m.
- impact pile driver type: Delmag D180-32 (600 kJ rated energy; 176.6 kN ram weight).
- helmet weight: 35.3 kN (estimated as 20% of the ram weight).
- 20-30 strikes/minute with an estimated 960 strikes/pile (proposed 700 strikes/pile with additional strikes for conservatism), maximum one pile per site in a day.
- modelling of the per-strike field for the finals strikes, when the pile footing is at 50 m below the sediment line.
- piling barge noise is not included in the model.

Mitigation of pile driving noise with respect to marine aquatic ecology focuses on reducing potential impacts to fish such as those identified as VECs for this Project. It is assumed that benthic fish and invertebrates are less sensitive to pile driving noise impacts due to their lack of swim bladders, and will therefore be conservatively protected through any mitigative measures taken to protect fish with swim bladders. The main goal for mitigation of pile driving noise impact on marine aquatic ecology is to minimize as much as possible the noise from the pile driving source, reducing the zone of potential impact and therefore reducing the likelihood of noise interaction. Attenuation results for piling mitigation with sound reduction ranging from 12-20 dB is assumed in the model for this Project. These reductions may be achieved with various proven technologies. Mitigation measures capable of achieving these sound reductions that may be considered for this Project include cofferdams, confined bubble curtains or double walled steel piles.

Appendix A summarizes all project and study assumptions.

2. Methods

For impulsive sounds from impact pile driving, time-domain representations of the pressure waves generated in the water are required to calculate sound pressure level (SPL), sound exposure level (SEL), and peak sound pressure level.

The source signatures of each pile are predicted using a finite-difference model that determines the physical vibration of the pile caused by hammer impact. The sound field radiating from the pile is simulated using a vertical array of point sources. Sound is itself a vibration wave associated with the oscillation of water particles. Modelling sound in the water column is inherently an evaluation of vibration.

A full-wave numerical sound propagation model was used to simulate the transmission of impact pile driving noise through water-saturated soils into water. For this study, synthetic pressure waveforms were computed using a Full Waveform Range-dependent Acoustic Model (FWRAM), which is JASCO's time-domain acoustic propagation model.

Sound propagation modelling considered, site-specific environmental data that describes the bathymetry, water sound speed, and seabed geoacoustics in the Fraser River.

The sound level estimates are presented in contour maps for non-mitigated case (Figure 10 to Figure 14) and with mitigation effect (Figure 15 to Figure 19). The contour maps show the planar distribution of the limits of the areas affected by levels higher than specific sound level thresholds. The results are also presented as ranges from the source to threshold sound levels and sizes of the affected areas both with mitigation and without mitigation in Table 6 to Table 11.

2.1. Acoustic Environment

2.1.1. Bathymetry

A bathymetry grid for the acoustic propagation model was compiled using isobath contour lines with 0.5 m depth and an extent of approximately 1000 m up and downstream the Fraser River from the proposed bridge crossing. The contour line data set was created by Northwest Hydraulic Consultants using a bathymetry grid compiled from various bathymetrical data sets collected in 2011 and 2014.

The vertices of the bathymetry contour lines were converted to point-data and assigned the depth value of the corresponding contour. The point data were averaged within 5 m cells and gridded using a minimum curvature method to produce the bathymetry grid with cell size of 5 m. The extent is equal to the original extent of the isobath contour lines (Figure 3).

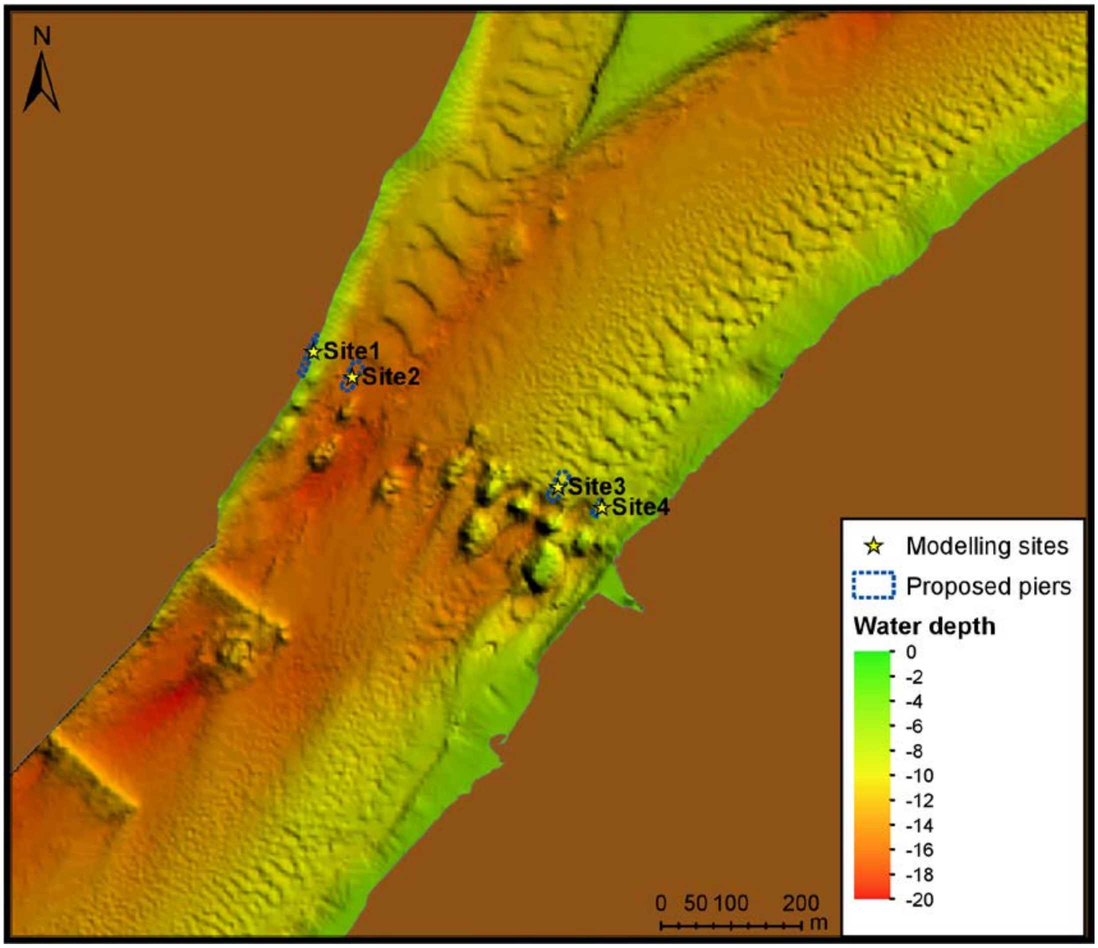

Figure 3. Riverbed relief in the vicinity of the Project area with marked footprints of the proposed in-river piers and pile driving modelling sites.

2.1.2. Geoacoustics

In shallow water environments where there is increased interaction with the seafloor, the properties of the substrate have a large influence over the sound propagation. The dominant soil type was assumed to be sandy silt. Table 1 presents the sediment layer geoacoustic property profile, which was estimated based on the sediment type and generic porosity-depth profile using a sediment grain-shearing model (Buckingham 2005).

Table 1. Estimated geoacoustic properties used for modelling, as a function of depth, in metres below the riverbed. Within an indicated depth range, the parameter varies linearly within the stated range.

Depth below riverbed (m)	Material	Density (g/cm^3)	P-wave speed (m/s)	P-wave attenuation (dB/λ)	S-wave speed (m/s)	S-wave attenuation (dB/λ)
0–5		1.44–1.52	1540–1590	0.32–0.53		
5–20			1590–11670	0.53–0.81		
20–50	Silty sand	1.52	1670–1750	0.81–1.06	150	3.65
50–100			1750–1820	1.06–1.28		
> 100			1820	1.28		

2.1.3. Sound Velocity Profile

A uniform sound velocity was assumed for the entire water column. Water turbulence in river environments does not allow stratification, as is typically observed in marine settings. The value of the sound velocity was derived using the empirical Marczaks equation (Marczak 1997) for fresh water:

$$c = 1.402\times10^{3} + 5.039\times T - 5.799\times10^{-2}\times T^{2} + 3.287\times10^{-4}\times T^{3} - 1.399\times10^{-6}\times T^{4} + 2.788\times10^{-9}\times T^{5}$$

The estimated sound velocity in water at the study location is approximately 1457 m/s based on the average water temperature of 10 °C from late summer to early spring. Average seasonal water temperature values were obtained from the DFO Fraser River Environmental Watch Report (DFO 2013).

2.2. Modelling Locations

Four sites, one at each in-river pier location, were selected for sound field modelling during pile driving operation (Figure 3). The water depths at the site locations were extracted from the grid representing the river bottom relief for the sound propagation modelling. Water depths at the sites vary from 1.1 m at the Eastern secondary pillar to 19.2 m at the Eastern main pillar (Table 2).

In addition, a composite scenario was included to represent the sound fields generated by pile driving operations occurring at multiple locations at the same time. Sites 2 & 3 were selected for this purpose to provide the most conservative estimate for simultaneous pile driving.

Table 2. Locations of the piling activities in UTM coordinates system (datum WGS84, zone 10).

Designation	Site	UTM zone 10		Water depth (m)
		Easting (m)	Northing (m)	
Eastern secondary pillar	1	507,511	5,450,777	1.1
Eastern main pillar	2	507,562	5,450,744	19.2
Western main pillar	3	507,855	5,450,588	9.6
Western secondary pillar	4	507,918	5,450,559	6.7

2.3. Acoustic Modelling Methods

The modelling of the acoustic fields around the pile driving operation was completed in two steps:

1. Modelling the acoustic signature of the source.
2. Propagation modelling of the acoustic signature of the source.

A pile generates acoustic waves along its whole length. In this study, each pile is represented by a series of monopole acoustic sources, each of which represents the acoustic radiation of a small vertical segment of the pile. The monopole sources are distributed along the entire pile length including the in-sediment section.

All modelling was conducted assuming that the bottom tip of the pile was near the target penetration depth (50 m below the sediment line).

2.3.1. Finite Difference Source Model

A physical model of pile vibration and near-field sound radiation was used to calculate the source levels of the piles. The physical model employed in this study computes the underwater vibration and sound radiation of a pile by solving the theoretical equations of motion for axial and radial vibrations of a cylindrical shell. These equations of motion are solved subject to boundary conditions, which describe the forcing function of the hammer at the top of the pile and the soil resistance at the base of the pile (Figure 4). Damping of the pile vibration due to radiation loading is computed for Mach waves emanating from the pile wall. The equations of motion are discretized using the finite difference (FD) method and are solved on a discrete time and depth mesh.

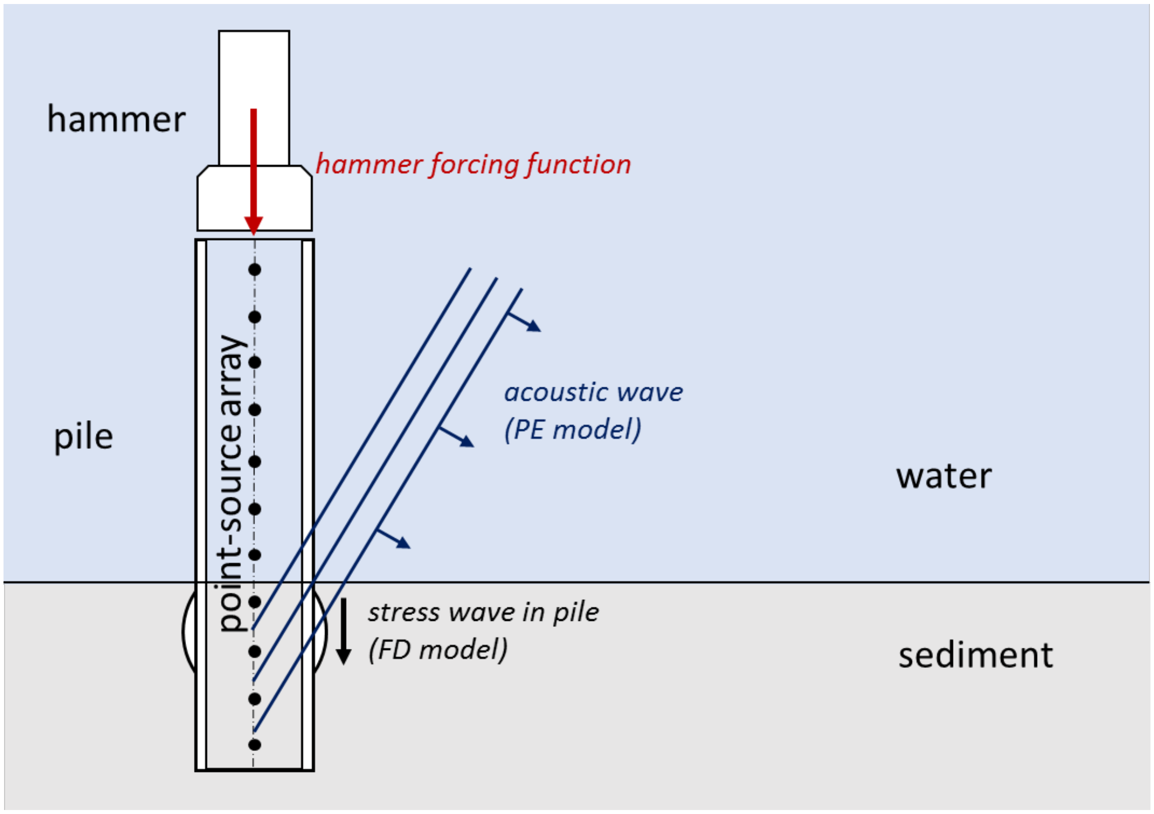

Figure 4. Physical model geometry for impact driving of a cylindrical pile (vertical cross-section). The hammer forcing function is used with the finite difference (FD) model to compute stress wave vibration in the pile. A vertical array of point sources is used with the parabolic equation (PE) model to compute the acoustic waves radiated by the pile wall.

The sound radiation from the pile itself is simulated using a vertical array of discrete point sources. The point sources are centred on the pile. Their amplitudes are derived using an inverse technique, such that their collective particle velocity—calculated using a near-field wave-number integration model—matches the particle velocity in water at the pile wall. The sound field from the vertical source array is calculated using a time-domain acoustic propagation model (Section 2.3.2). A detailed description of the theory behind the physical model is provided in MacGillivray (2014). The accuracy of JASCO's pile driving model has been verified by comparing its output against benchmark scenarios (Lippert et al. 2016).

To model the sound emissions of the piles, it was first necessary to model the impact force of the pile driving hammers. The exact model of the pile driver was not available for this study, so a suitable model was selected by JASCO based on experience with previous acoustic modelling projects involving pile driving operations. The selected pile driver was a Delmag D180-32 diesel impact pile driver with rated energy of 600 kJ.

The force at the top of each pile, associated with the proposed hammers, was computed using the GRLWEAP 2010 wave equation model (GRLWEAP, Pile Dynamics 2010), which includes a large database of various hammers. The database integrated into GRLWEAP contains parameters of the pile drivers that are required for the modelling of the forcing function.

Forcing function for the hammer was modelled assuming that driving was carried out using the maximum recommended hammer energy (Figure 5). The forcing functions were computed assuming direct contact between the hammer and the piles (i.e., no cushion material). The FD model was then used to compute the resulting pile vibrations. The stress wave generated at the top of the pile by the hammer travels downward to the pile toe, where it is partially reflected. The reflected stress waves travel up and down the pile and are gradually dissipated by soil resistance and radiative damping.

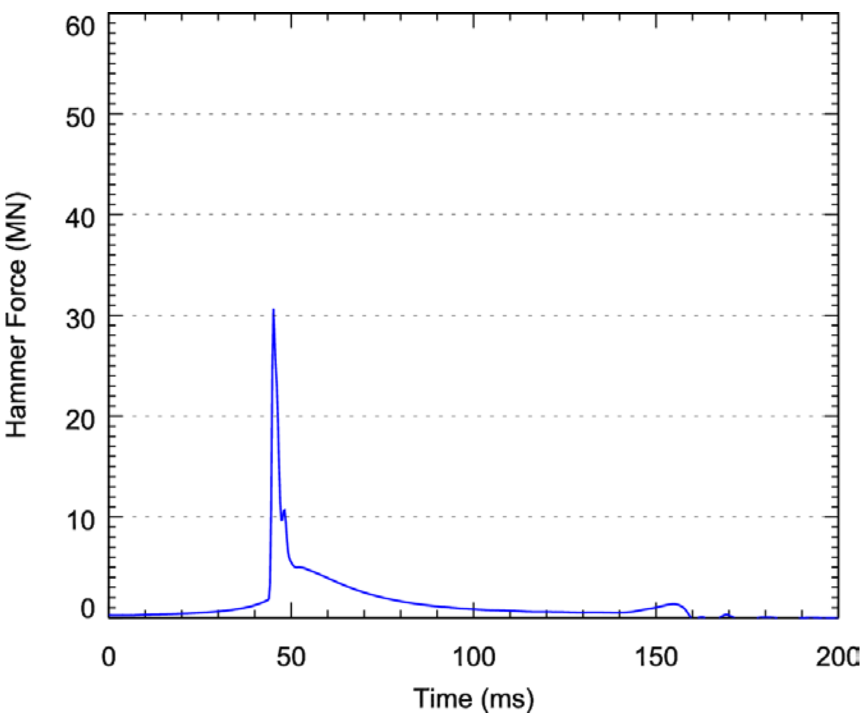

Figure 5. Modelled forcing functions versus time for the Delmag D180-32 diesel impact hammer for a 180 cm pile.

To model the sound waves associated with the pile vibration in an acoustic propagation model, the piles were represented as vertical arrays of discrete point-sources. Pressure signatures for the point-sources were computed from the particle velocity at the pile wall up to a maximum frequency of 2048 Hz. This frequency range was deemed suitable, since most of the sound energy generated by the piles was below 1000 Hz. Figure 6 is an example of spectral density of the signatures for three discrete sources within an array of monopole sources representing the pile at Site 2. The discrete sources were distributed through the whole length of the pile of 69 m (50 m in the sediment plus 19 m in the water column) with vertical separation of 0.25 m. The same vertical step was used for the piles at the other three sites. The length of the pile was adjusted for the site-specific water depth. The section length of the pile within the sediment was constant at each site. The pile source signature modelling was carried out for each modelling site individually.

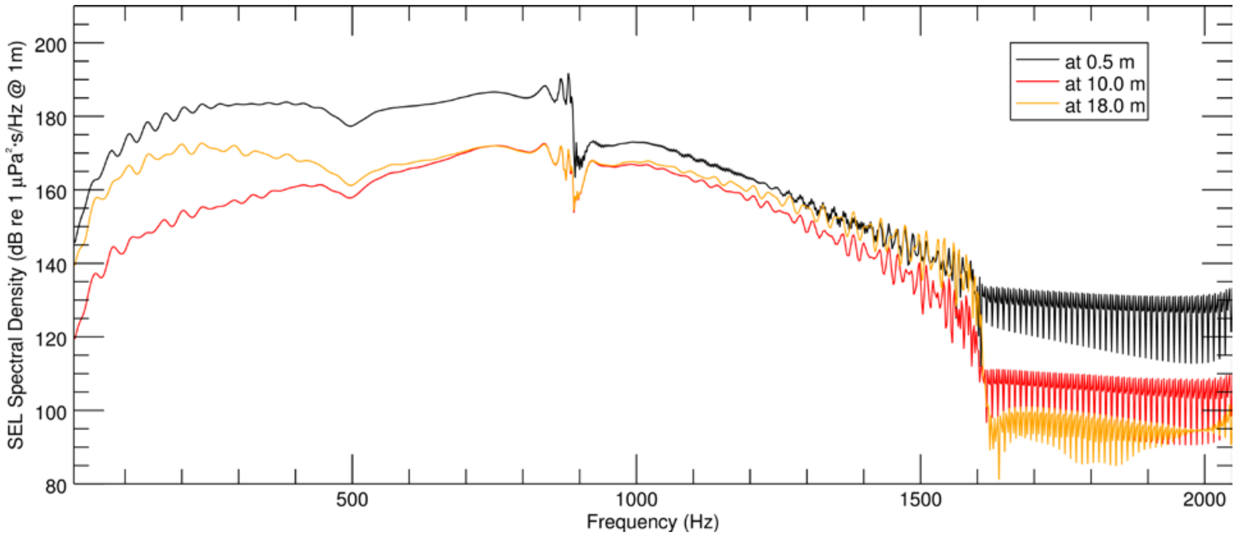

Figure 6. Example of SEL spectral density of acoustic point source signatures calculated by the FD model. Spectra are shown for monopole sources of Pile 2 at specified depth below the water surface (180 cm pile diameter, 50 m penetration, 600 kJ hammer).

2.3.2. Noise Propagation Modelling with FWRAM

For impulsive sounds from impact pile driving, time-domain representations of the pressure waves generated in the water are required to calculate root-mean-square sound pressure level (rms SPL) and peak SPL. Furthermore, the pile must be represented as a distributed source to accurately characterise vertical directivity effects in the near-field zone. Synthetic pressure waveforms were computed using FWRAM, which is a time-domain acoustic model based on a wide-angle parabolic equation algorithm. FWRAM computes synthetic pressure waveforms versus range and depth for range-varying marine acoustic environments. FWRAM computes pressure waveforms via Fourier synthesis of the modelled acoustic transfer function in closely spaced frequency bands. FWRAM employs the array starter method to accurately model sound propagation from a spatially distributed source, and accounts for re-radiation of ground-borne vibration waves into water (MacGillivray and Chapman 2012).

Synthetic pressure waveforms were modelled over the frequency range 10–2048 Hz, inside a 500 ms window (Figure 7).

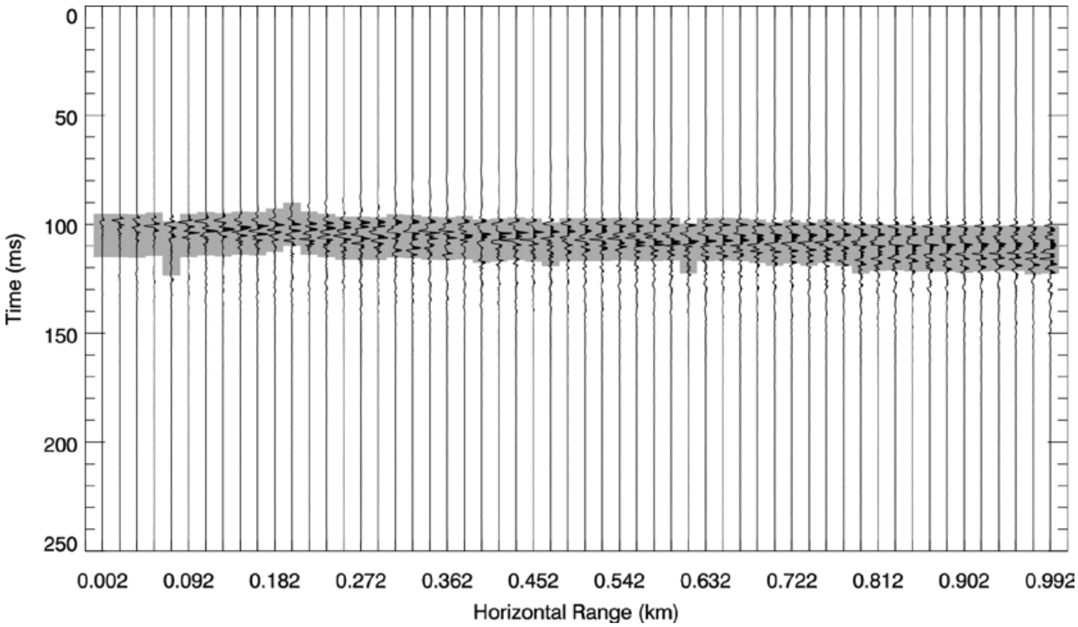

Figure 7. Example of synthetic pressure waveforms computed by FWRAM for a pile at multiple range offsets. Site 2, propagation profile azimuth: 54°, receiver depth: 10 m. For display purposes, the amplitudes of the pressure traces have been normalized and the starting time of the pulse is corrected for sound travel time.

2.3.3. *N*×2-D Volume Approximation

FWRAM computes acoustic fields in three dimensions by modelling transmission loss within two-dimensional (2-D) vertical planes aligned along radials covering a 360° swath from the source, an approach commonly referred to as *N*×2-D. These vertical radial planes are separated by an angular step size of $\Delta\theta$, yielding $N = 360°/\Delta\theta$ number of planes (Figure 8).

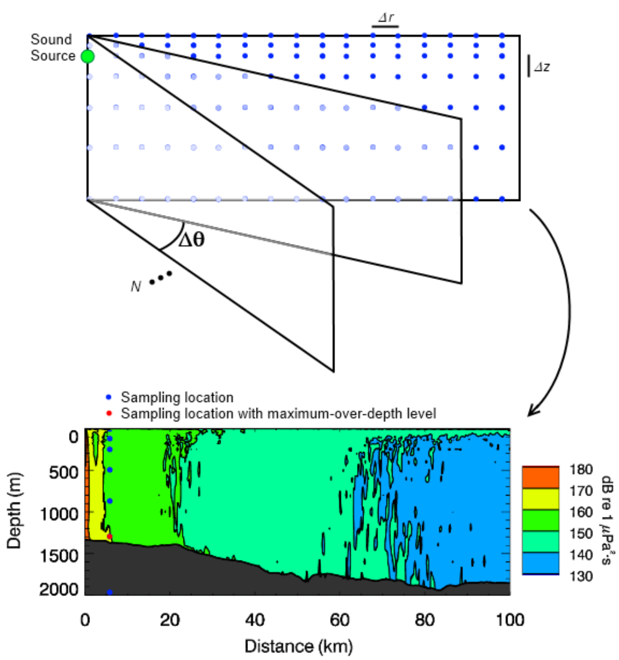

Figure 8. The *N*×2-D and maximum-over-depth modelling approach.

Acoustic propagation was modelled along sixty radials with corresponding 6° angular steps ($\Delta\theta$). The horizontal step size (Δr) for the distributed virtual receivers was 2 m. Vertically, the virtual receivers were positioned every 1 m from 1 m to 27 m below the water surface. Sound level contours were based only on virtual receivers located in the water column. The output from the acoustic propagation modelling is a series of synthetic traces, one per virtual receiver. Calculations are performed on each synthetic trace yielding three acoustic metrics: peak SPL, rms SPL, and SEL at each virtual receiver. The complete set of all virtual receivers forms a cylindrical grid to represent the acoustic field in the specific metric around the pile.

2.4. Radii and Area Calculation

The vertical dimension of the cylindrical grids representing the acoustic fields around the piles is reduced using the maximum-over-depth rule (i.e., the received sound level at each point in the horizontal plane is taken to be the maximum value over all modelled depths for that point). This provides a conservative prediction of the received sound level around the source, independent of depth. The resultant N×1-D dataset representing the acoustic field in the horizontal plain was gridded using a triangulation method onto a 2-D Cartesian grid with a 2 m cell size. Prior to gridding, smoothing was applied to the data points along each individual 1-D radial. The smoothing method was a boxcar average with a width of ten data points. The data points within the smoothing width window from the source were not subject to smoothing.

Ranges to specific thresholds were calculated (Section 3.1) and maps of the horizontal acoustic field footprints were plotted (Section 3.2) based on a 2-D Cartesian grid representing horizontal distribution of the acoustic field around a source.

Two ranges relative to the source are reported for each sound level:

- R_{max}, the maximum range at which the given sound level is reached in the modelled maximum-over-depth sound field.
- $R_{95\%}$, the maximum range at which the given sound level is reached after the 5% farthest such points are excluded (Figure 9).

The $R_{95\%}$ is used because the maximum-over-depth sound field footprint might not be circular and, along a few azimuths, could extend far beyond the main ensonification zone. Regardless of the geometric shape of the maximum-over-depth footprint, $R_{95\%}$ is the predicted range encompassing at least 95% of the area (in the horizontal plane) that would be exposed to sound at or above that level. The difference between R_{max} and $R_{95\%}$ depends on the source directivity and the heterogeneity of the acoustic environment. The $R_{95\%}$ excludes the ends of protruding areas and small isolated acoustic foci that are non-representative of the nominal ensonification zone.

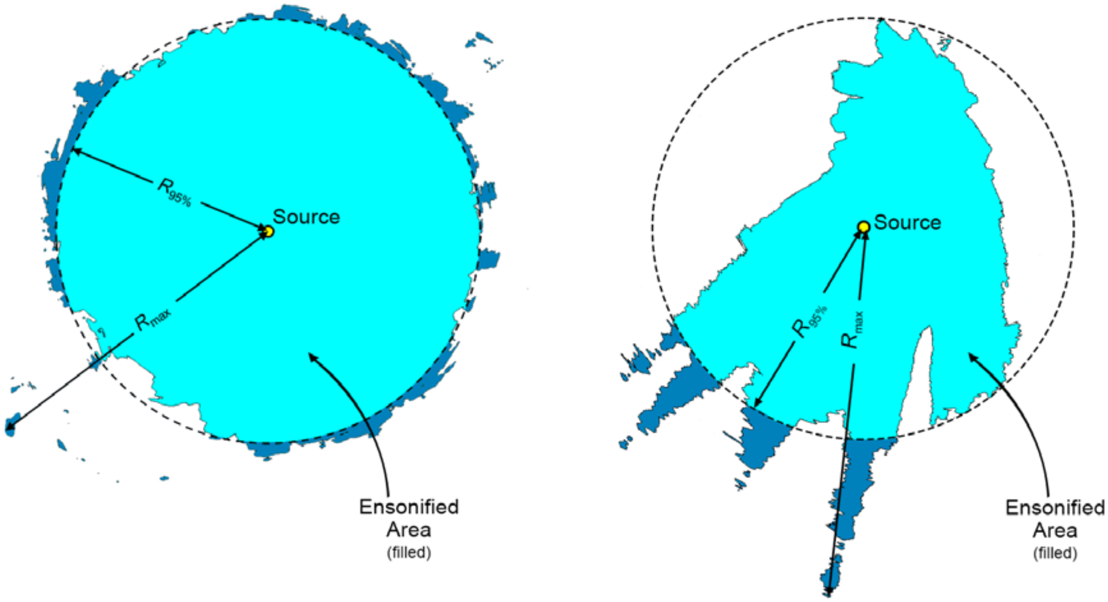

Figure 9. Sample areas ensonified to an arbitrary sound level with R_{max} and R95% ranges shown for two different scenarios. (a) Largely symmetric sound level contour with small protrusions. (b) Strongly asymmetric sound level contour with long protrusions. Light blue indicates the ensonified areas bounded by $R_{95\%}$; darker blue indicates the areas outside this boundary which determine R_{max}.

In addition to radii, an affected area was calculated for each threshold of interest. The area was calculated based on the 2-D Cartesian grid by counting the number of cells with values above specific thresholds and multiplying the value by the cell size. The affected area value can be combined with animal distribution for estimating the number of affected animals. Also, the consideration of the affected area is suitable for assessment of the exposure from a composite scenario with multiple acoustic sources, where the separation distance of the sources is comparable with the threshold radii from a single source.

2.5. Acoustic Thresholds

To assess the potential impacts of a sound-producing activity, it is necessary to first establish exposure criteria for which sound levels may be expected to have a negative impact on animals. A technical report by an American National Standards Institute (ANSI)-registered committee (Popper et al. 2014) reviewed available data and suggested metrics and methods for estimating acoustic impacts for fish, fish eggs and larvae, and sea turtles. Fish are classified based on their hearing capabilities typically determined by the presence of a swim bladder and whether it is directly used in hearing (note that salmonids and sturgeon have swim bladders that are not involved in hearing). Threshold levels suggested by Popper et al. (2014) for mortality, potential mortal injury, and recoverable injury for pile driving sounds are shown in Table 3. The report does not define sound levels that may result in behavioural response, but does indicate a high likelihood of response near pile driving (tens of metres), moderate response at intermediate ranges (hundreds of metres), and low response far (thousands of metres) from the pile (Popper et al. 2014). Ranges to the listed thresholds were computed for the Project.

The thresholds for SEL were defined for exposure accumulated over multiple acoustic events (strikes) occurring in a 24-hour period. Guidelines are for the lowest level where injury was found (Table 3).

Table 3. Peak SPL and SEL dual criteria thresholds for acoustic effects on fish (adapted from Popper et al. (2014).

Fish Group	Impulsive Signals			
	Mortality and Potential Mortal Injury		Recoverable Injury	
	SEL_{24hr} (dB re 1 µPa²·s)	SPL_{pk} (dB re 1 µPa)	SEL_{24hr} (dB re 1 µPa²·s)	SPL_{pk} (dB re 1 µPa)
Fish without swim bladder	>219	>213	>216	>213
Fish with swim bladder not involved in hearing	210	>207	203	>207
Fish with swim bladder involved in hearing	207	>207	203	>207
Eggs and larvae	>210	>207	(N) Moderate (I) Low (F) Low	

Notes: SEL_{24hr} = sound exposure level based on accumulated exposure over 24-hour period; SPL_{pk} = peak sound pressure level. Relative risk (high, moderate, low) is given for animals at three distances from the source defined in relative terms as near (N), intermediate (I), and far (F).

2.6. Mitigation

Several studies have been conducted to determine the efficacy of various mitigation techniques for reducing sound output from piling installation, including double-walled steel piling, cofferdams, and bubble curtains. The methods employed in these studies involves the measurement of received sound levels in the water column during unmitigated and mitigated pile driving. The results of these studies demonstrate variability in sound reduction. Reinhall et al. (2015) focused on a double-walled pile consisting of two concentric tubes connected by a special driving shoe, with an air gap between the two tubes. The double walled pile is driven into the sediment by using traditional equipment to strike the inner tube only. The air gap between the inner and outer tube prevents the radial deformation wave produced by the pile hammer from interacting with the water and the sediment. In one embodiment of the double pile design the inner tube can be removed and repeatedly reused (Reinhall et al. 2015).

Reinhall et al. (2015) conducted a field test of the double-walled pile in Puget Sound, Washington, to estimate the level of mitigation using this configuration. The test measurements were performed on the 762 mm piles that were driven using a conventional pile driving method with no mitigation measure applied and the piles driven with doubled-wall mitigation. The test report provided a set of broadband level reduction values due to mitigation at different distances from the pile.

Other studies have assessed other double-walled pile technologies, bubble curtain technologies, cofferdams, and combinations of these mitigations for sound attenuation, with reductions in decibel level varying between 6 and 23 dB (Reinhall et al. 2015, Christopherson and Lundberg 2013, Bellmann 2014).

To estimate the extent of the thresholds during mitigated Project activities, the reduction values reported by Reinhall et al. (2015) were applied to the unmitigated modelled sound levels. To account for the uncertainty of the method, the reported minimum and maximum reduction values for each of the metric were considered (Table 4).

Table 4. Minimum and maximum reduction values due to mitigation for a doubled wall mitigation technique (Reinhall et al. 2015).

Metric	Minimum reduction	Maximum reduction
SEL	13.8 dB	17.2 dB
Peak SPL	12.0 dB	21.2 dB

The reduction values were applied to the SEL and peak SPL broadband sound fields providing two sets of mitigated sound levels for each metric. Threshold radii and contours were generated for the best case and worst case scenarios using maximum and minimum reduction values derived from the Reinhall et al. (2015) field test.

2.7. Scenarios Modelled

To assess the potential sound exposure and sound pressure levels that might result from various activity combinations, several scenarios were modelled with and without mitigation.

Table 5. Modelling scenarios used to calculate potential acoustic fields. Reference Figure 3 for site locations. All scenarios use 1800 mm diameter piles and are calculated with and without mitigation.

Scenarios	Site 1	Site 2	Site 3	Site 4
1		X		
2			X	
3	X	X		
4		X	X	
5			X	X
6	X	X	X	X

3. Results

The acoustic fields were modelled for all the scenarios listed in Table 5. The ranges to specific thresholds are reported for each scenario. The threshold contour maps are provided for the worst case (the largest acoustic footprint) out of the four individual pier sites and for several combined scenarios, including the assumed worst case of simultaneous pile driving at four pier locations.

The results are presented for two single pile scenarios and four multi-pile scenarios. Single pile scenarios assume that only one pile is being driven in a given time period within the project area. Multi-pile scenarios assume that multiple piles are being driven concurrently within the project area, one pile per site. The acoustic field for multi-pile scenarios was calculated from the superposition of the fields from single pile scenarios. The combined SEL field was calculated by addition of the SEL fields from each individual pile. The combined peak SPL field was obtained by taking the maximum level of the peak SPL fields from each individual pile.

The peak sound pressure level metric of the acoustic signal, as well as the SEL were calculated directly from the modelled synthetic pressure waveforms.

Accumulated SEL over a 24-hour period was calculated based on the modelled SEL for a single pile strike:

$$SEL_{24hr} = SEL_{(\text{1-blow})} + 10\log_{10} N \qquad (1)$$

where *N* is the estimated number of strikes that would occur in a 24-hour period. The number of strikes used to estimate the SEL_{24hr} for a single site was 1000, which is 300 strikes more than estimated number of strikes required to complete installation of one pile for the Project. The addition of strikes accounts for uncertainty at this early stage of the Project and is considered a conservative assumption. The increase in the SEL from the additional 300 strikes is 1.5 dB.

3.1. Tables of Threshold Ranges

Calculated distances to specific thresholds were based on maximum sound level over the entire water column (maximum-over-depth approach). Maximum (R_{max}, m) and 95% ($R_{95\%}$, m) horizontal distances as well as ensonified area (A, $m^2 \times 10^3$) are reported for each criterion (see Section 2.5). The SEL was calculated in the frequency range from 10 to 2000 Hz without any filtering applied.

Table 6 and Table 7 provide estimated threshold distances for impact pile driving with the D180-32 hammer performed at Site 2 and Site 3, respectively. Threshold distances for multi-pile scenarios Site 1 + Site 2 (Table 8), Site 2 + Site 3 (Table 9), Site 3 + Site 4 (Table 10), and for simultaneous pile driving at all four sites (Table 11) are also provided.

The ranges to the thresholds for the multi-pile scenarios were calculated using two approaches, based on the extension of the threshold contours. If the threshold contours feature disconnected areas around each site then the ranges were calculated for each area separately relative to the respective site. The greatest value was reported in the table. If the threshold contour formed a continuous area that encompassed both sites, then the ranges were calculated relative to the mid-point between the two sites. The approach used in the calculation of the values is indicated in the radii table.

In all cases the ensonified area value was calculated based on the entire area encompassed by the threshold contour.

For each threshold, three sets of values are provided representing the unmitigated case and two mitigated scenarios with minimum and maximum reduction (see Table 4 and Table 5).

Table 6. Site 2: Ranges (R_{max} and $R_{95\%}$ in metres) and affected area (A in $m^2 \times 10^3$) for specific injury thresholds for the D180-32 hammer. For eggs and larvae refer to Fish with swim bladder not involved in hearing as they have equivalent threshold levels.

Species	Metric	Threshold (dB)	no mitigation			min reduction			max reduction		
			R_{max}	$R_{95\%}$	*A*	R_{max}	$R_{95\%}$	*A*	R_{max}	$R_{95\%}$	*A*
Mortality and Potential Mortal Injury											
Fish without swim bladder	SEL_{24hr}	219	27	25	1.81	—	—	—	—	—	—
	SPL_{pk}	213	63	56	7.24	10	10	0.31	—	—	—
Fish with swim bladder not involved in hearing	SEL_{24hr}	210	113	103	13.3	11	11	0.38	7	6	0.15
	SPL_{pk}	207	201	175	42.3	27	24	1.66	4	4	0.05
Fish with swim bladder involved in hearing	SEL_{24hr}	207	201	167	42.3	16	15	0.71	11	11	0.38
	SPL_{pk}	207	201	175	42.3	27	24	1.66	4	4	0.05
Recoverable injury											
Fish without swim bladder	SEL_{24hr}	216	48	43	4.8	—	—	—	—	—	—
	SPL_{pk}	213	63	56	7.2	10	10	0.31	—	—	—
Fish with swim bladder	SEL_{24hr}	203	304	234	103	45	40	4.1	18	17	0.91
	SPL_{pk}	207	201	175	42.3	27	24	1.66	4	4	0.05

Table 7. Site 3: Ranges (R_{max} and $R_{95\%}$ in metres) and affected area (A in $m^2 \times 10^3$) for specific injury thresholds for the D180-32 hammer. For eggs and larvae refer to Fish with swim bladder not involved in hearing as they have equivalent threshold levels.

Species	Metric	Threshold (dB)	no mitigation			min reduction			max reduction		
			R_{max}	$R_{95\%}$	*A*	R_{max}	$R_{95\%}$	*A*	R_{max}	$R_{95\%}$	*A*
Mortality and Potential Mortal Injury											
Fish without swim bladder	SEL_{24hr}	219	21	19	1.26	—	—	—	—	—	—
	SPL_{pk}	213	51	42	4.3	10	10	0.31	—	—	—
Fish with swim bladder not involved in hearing	SEL_{24hr}	210	73	57	8.17	12	11	0.45	8	8	0.20
	SPL_{pk}	207	127	100	22.7	22	21	1.4	5	5	0.08
Fish with swim bladder involved in hearing	SEL_{24hr}	207	123	98	26.6	17	16	0.91	11	11	0.45
	SPL_{pk}	207	127	100	22.7	22	21	1.4	5	5	0.08
Recoverable injury											
Fish without swim bladder	SEL_{24hr}	216	31	28	2.3	—	—	—	—	—	—
	SPL_{pk}	213	51	42	4.3	10	10	0.31	—	—	—
Fish with swim bladder	SEL_{24hr}	203	291	207	74.5	28	26	2.1	18	17	1.0
	SPL_{pk}	207	127	100	22.7	22	21	1.4	5	5	0.08

Table 8. Site 1 + Site 2: Ranges (R_{max} and $R_{95\%}$ in metres) and affected area (A in $m^2 \times 10^3$) for specific injury thresholds for the D180-32 hammer. For eggs and larvae refer to Fish with swim bladder not involved in hearing as they have equivalent threshold levels. The ranges are provided relative to Site 2.

Species	Metric	Threshold (dB)	no mitigation			min reduction			max reduction		
			R_{max}	$R_{95\%}$	*A*	R_{max}	$R_{95\%}$	*A*	R_{max}	$R_{95\%}$	*A*
Mortality and Potential Mortal Injury											
Fish without swim bladder	SEL_{24hr}	219	30	27	2.46	—	—	—	—	—	—
	SPL_{pk}	213	63	56	8.2	10	10	0.31	—	—	—
Fish with swim bladder not involved in hearing	SEL_{24hr}	210	123	111	22.7	11	11	0.53	7	6	0.15
	SPL_{pk}	207	201	175	43.7	27	24	1.96	4	4	0.05
Fish with swim bladder involved in hearing	SEL_{24hr}	207	210	180	55.6	16	16	1.02	11	11	0.45
	SPL_{pk}	207	201	175	43.7	27	24	1.96	4	4	0.05
Recoverable injury											
Fish without swim bladder	SEL_{24hr}	216	49	44	5.8	—	—	—	—	—	—
	SPL_{pk}	213	63	56	8.2	10	10	0.31	—	—	—
Fish with swim bladder	SEL_{24hr}	203	318	274	140	46	41	5.03	19	18	1.26
	SPL_{pk}	207	201	175	43.7	27	24	1.96	4	4	0.05

Table 9. Site 2 + Site 3: Ranges (R_{max} and $R_{95\%}$ in metres) and affected area (A in $m^2 \times 10^3$) for specific injury thresholds for the D180-32 hammer. For eggs and larvae refer to Fish with swim bladder not involved in hearing as they have equivalent threshold levels. The ranges are provided relative to Site 2 unless otherwise noted.

Species	Metric	Threshold (dB)	no mitigation			min reduction			max reduction		
			R_{max}	$R_{95\%}$	*A*	R_{max}	$R_{95\%}$	*A*	R_{max}	$R_{95\%}$	*A*
Mortality and Potential Mortal Injury											
Fish without swim bladder	SEL_{24hr}	219	28	26	3.02	—	—	—	—	—	—
	SPL_{pk}	213	63	56	11.3	10	10	0.62	—	—	—
Fish with swim bladder not involved in hearing	SEL_{24hr}	210	121	111	24.9	11	11	0.8	7	6	0.38
	SPL_{pk}	207	201	175	65.1	27	24	3.0	4	4	0.11
Fish with swim bladder involved in hearing	SEL_{24hr}	207	277[M]	238[M]	91.9	16	15	1.5	11	11	0.80
	SPL_{pk}	207	201	175	65.1	27	24	3.0	4	4	0.11
Recoverable injury											
Fish without swim bladder	SEL_{24hr}	216	48	44	7.2	—	—	—	—	—	—
	SPL_{pk}	213	63	56	11.3	10	10	0.62	—	—	—
Fish with swim bladder	SEL_{24hr}	203	430[M]	321[M]	231	45	40	6.1	18	17	1.96
	SPL_{pk}	207	201	175	65.1	27	24	3.0	4	4	0.11

[M])-radii are calculated relative to the mid-point between Site 2 and 3

Table 10. Site 3 + Site 4: Ranges (R_{max} and $R_{95\%}$ in metres) and affected area (A in m²×10³) for specific injury thresholds for the D180-32 hammer. For eggs and larvae refer to Fish with swim bladder not involved in hearing as they have equivalent threshold levels. The ranges are provided relative to Site 3.

Species	Metric	Threshold (dB)	no mitigation			min reduction			max reduction		
			R_{max}	$R_{95\%}$	*A*	R_{max}	$R_{95\%}$	*A*	R_{max}	$R_{95\%}$	*A*
Mortality and Potential Mortal Injury											
Fish without swim bladder	SEL_{24hr}	219	23	21	2.64	—	—	—	—	—	—
	SPL_{pk}	213	51	44	7.85	10	10	0.71	—	—	—
Fish with swim bladder not involved in hearing	SEL_{24hr}	210	126	109	24.9	12	12	0.91	8	8	0.45
	SPL_{pk}	207	134	120	30.8	22	21	2.46	5	5	0.2
Fish with swim bladder involved in hearing	SEL_{24hr}	207	174	138	55.6	17	16	1.66	11	11	0.8
	SPL_{pk}	207	134	120	30.8	22	21	2.46	5	5	0.2
Recoverable injury											
Fish without swim bladder	SEL_{24hr}	216	31	28	2.3	—	—	—	—	—	—
	SPL_{pk}	213	51	42	4.3	10	10	0.31	—	—	—
Fish with swim bladder	SEL_{24hr}	203	291	207	74.5	28	26	2.1	18	17	1.0
	SPL_{pk}	207	127	100	22.7	22	21	1.4	5	5	0.08

Table 11. All four sites: Ranges (R_{max} and $R_{95\%}$ in metres) and affected area (A in m²×10³) for specific injury thresholds for the D180-32 hammer. For eggs and larvae refer to Fish with swim bladder not involved in hearing as they have equivalent threshold levels. The ranges are provided relative to Site 2 unless otherwise noted.

Species	Metric	Threshold (dB)	no mitigation			min reduction			max reduction		
			R_{max}	$R_{95\%}$	*A*	R_{max}	$R_{95\%}$	*A*	R_{max}	$R_{95\%}$	*A*
Mortality and Potential Mortal Injury											
Fish without swim bladder	SEL_{24hr}	219	31	28	5.28	—	—	—	—	—	—
	SPL_{pk}	213	63	56	16.3	10	10	1.02	—	—	—
Fish with swim bladder not involved in hearing	SEL_{24hr}	210	176	123	56.4	11	11	1.39	7	6	0.62
	SPL_{pk}	207	201	176	74.5	27	24	4.54	4	4	0.25
Fish with swim bladder involved in hearing	SEL_{24hr}	207	314[M]	274[M]	149	16	16	2.83	11	11	1.26
	SPL_{pk}	207	201	176	74.5	27	24	4.54	4	4	0.25
Recoverable injury											
Fish without swim bladder	SEL_{24hr}	216	50	45	11.3	—	—	—	—	—	—
	SPL_{pk}	213	63	56	16.3	10	10	1.02	—	—	—
Fish with swim bladder	SEL_{24hr}	203	466[M]	356[M]	328	46	42	9.5	19	18	3.42
	SPL_{pk}	207	201	176	74.5	27	24	4.54	4	4	0.25

[M)]-radii are calculated relative to mid-point between Site 2 and 3

3.2. Maps of Threshold Contours

The maps provide threshold contours based on SEL and peak SPL fields for SEL for the D180-32 impact hammer for single pile scenario at Site 2 (Figure 10) and four multi-pile scenarios: Site 1 + Site 2 (Figure 11), Site 2 + Site 3 (Figure 12), Site 3 + Site 4 (Figure 13), and for simultaneous pile driving at all four sites (Figure 14).

The contours for the mitigated cases (minimum and maximum reduction) of the respective scenarios are provided in Figure 15 (Site 2), Figure 16 (Site 1 + Site 2), Figure 17 (Site 2 + Site 3), Figure 18 (Site 3 + Site 4), and Figure 19 (all four sites).

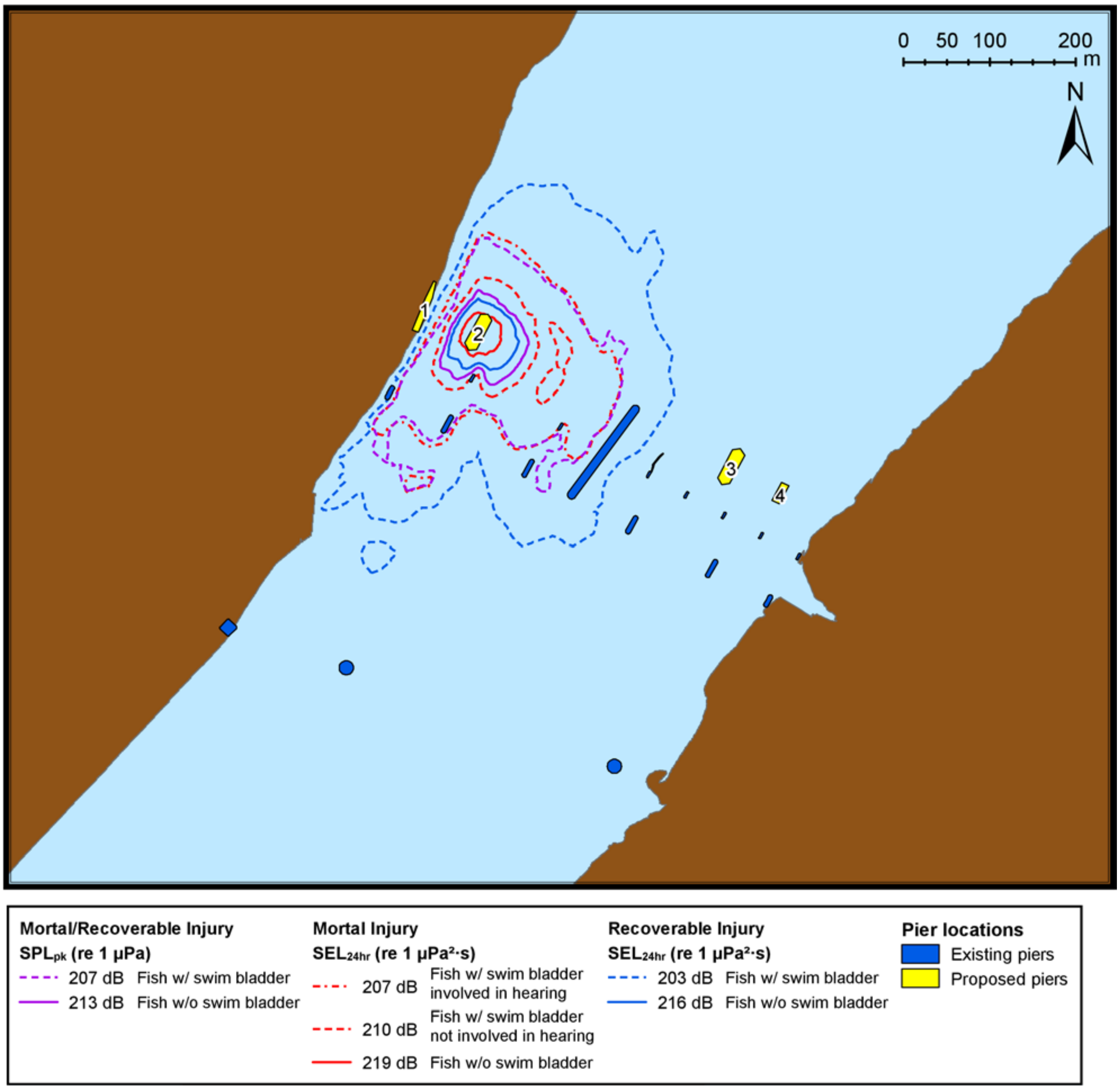

Figure 10. Site 2: Threshold contours based on maximum-over-depth acoustic fields for pile driving using D180-32 impact hammer.

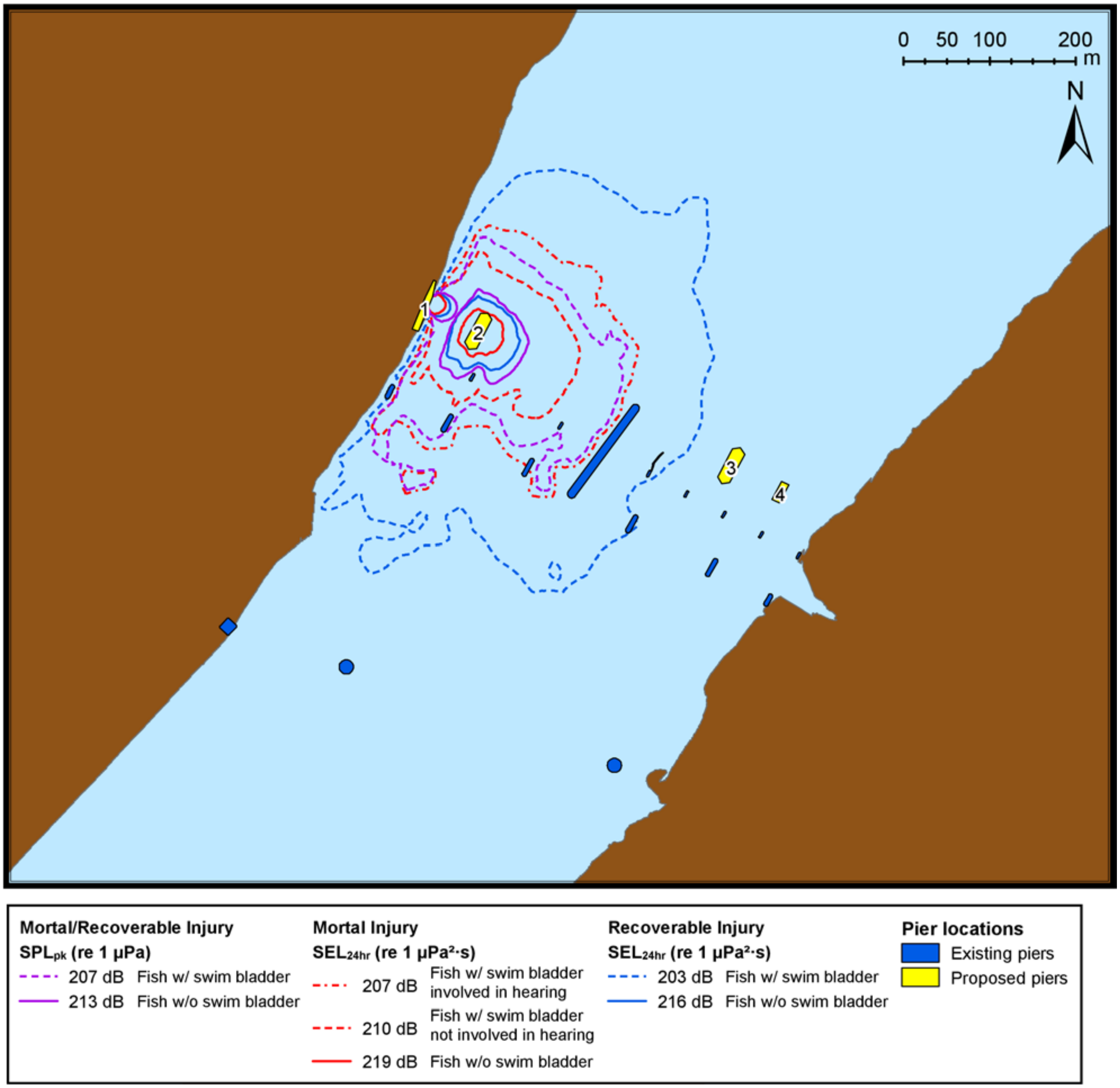
0 50 100 200
m
N
1
2
3
4
Mortal/Recoverable Injury
SPLpk (re 1 µPa)
207 dB Fish w/ swim bladder
213 dB Fish w/o swim bladder
Mortal Injury
SEL24hr (re 1 µPa²·s)
207 dB Fish w/ swim bladder involved in hearing
210 dB Fish w/ swim bladder not involved in hearing
219 dB Fish w/o swim bladder
Recoverable Injury
SEL24hr (re 1 µPa²·s)
203 dB Fish w/ swim bladder
216 dB Fish w/o swim bladder
Pier locations
Existing piers
Proposed piers

Figure 11. Multi-pile scenario Site 1 + Site 2: Threshold contours based on maximum-over-depth acoustic fields for pile driving using D180-32 impact hammer at Site 1 and 2 simultaneously.

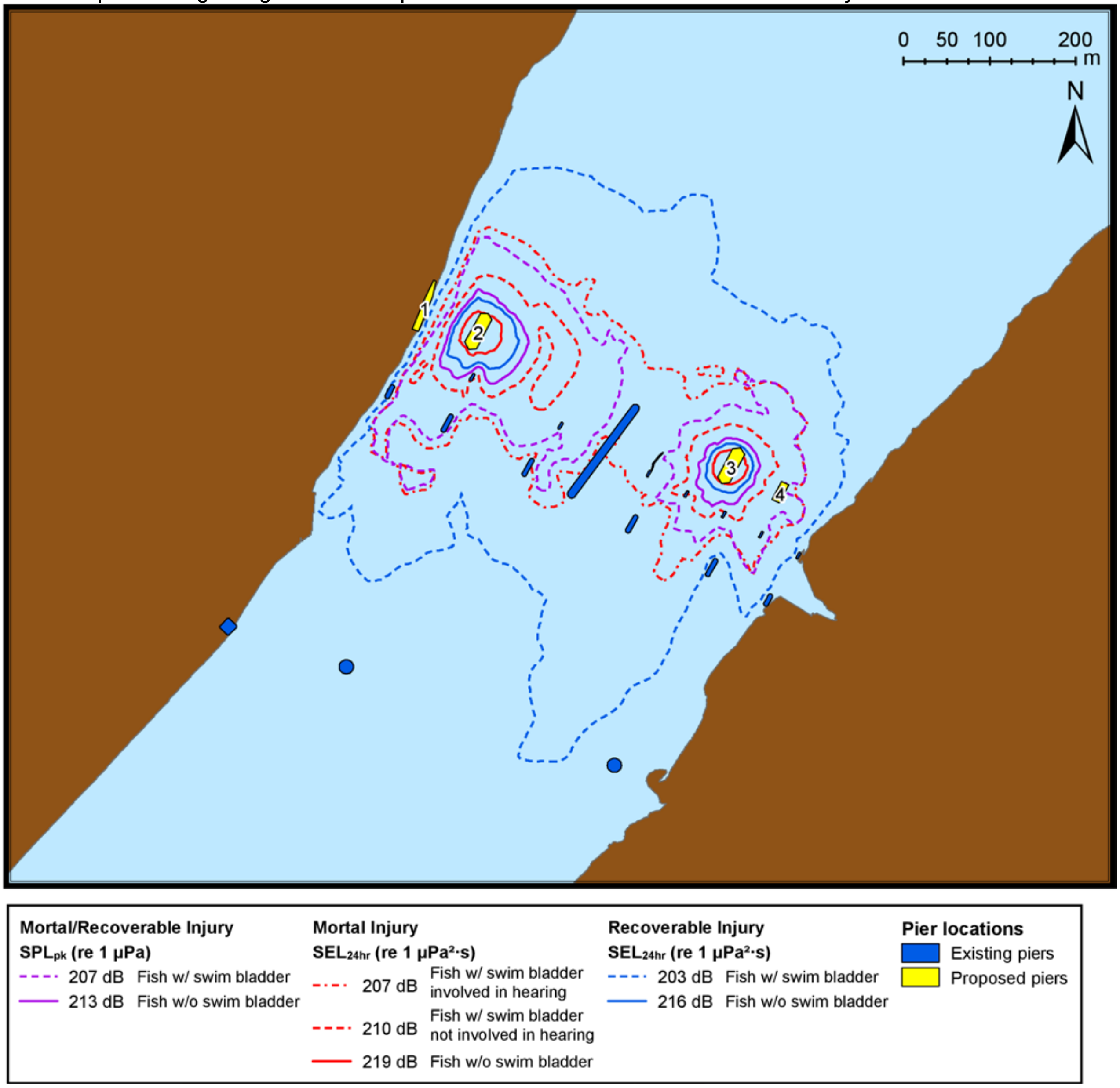

Figure 12. Multi-pile scenario Site 2 + Site 3: Threshold contours based on maximum-over-depth acoustic fields for pile driving using D180-32 impact hammer at Site 2 and 3 simultaneously.

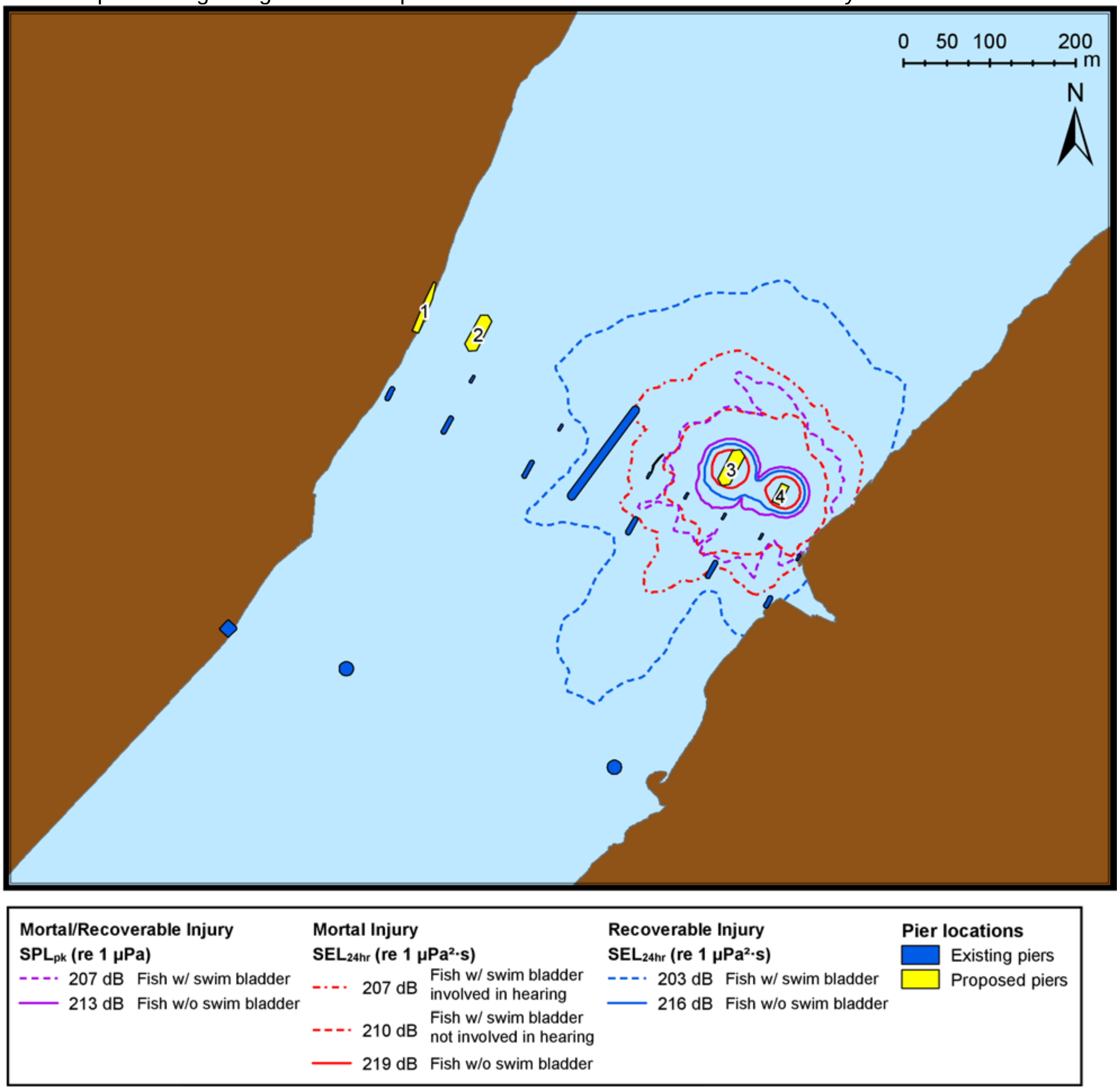

Figure 13. Multi-pile scenario Site 3 + Site 4: Threshold contours based on maximum-over-depth acoustic fields for pile driving using D180-32 impact hammer at Site 3 and 4 simultaneously.

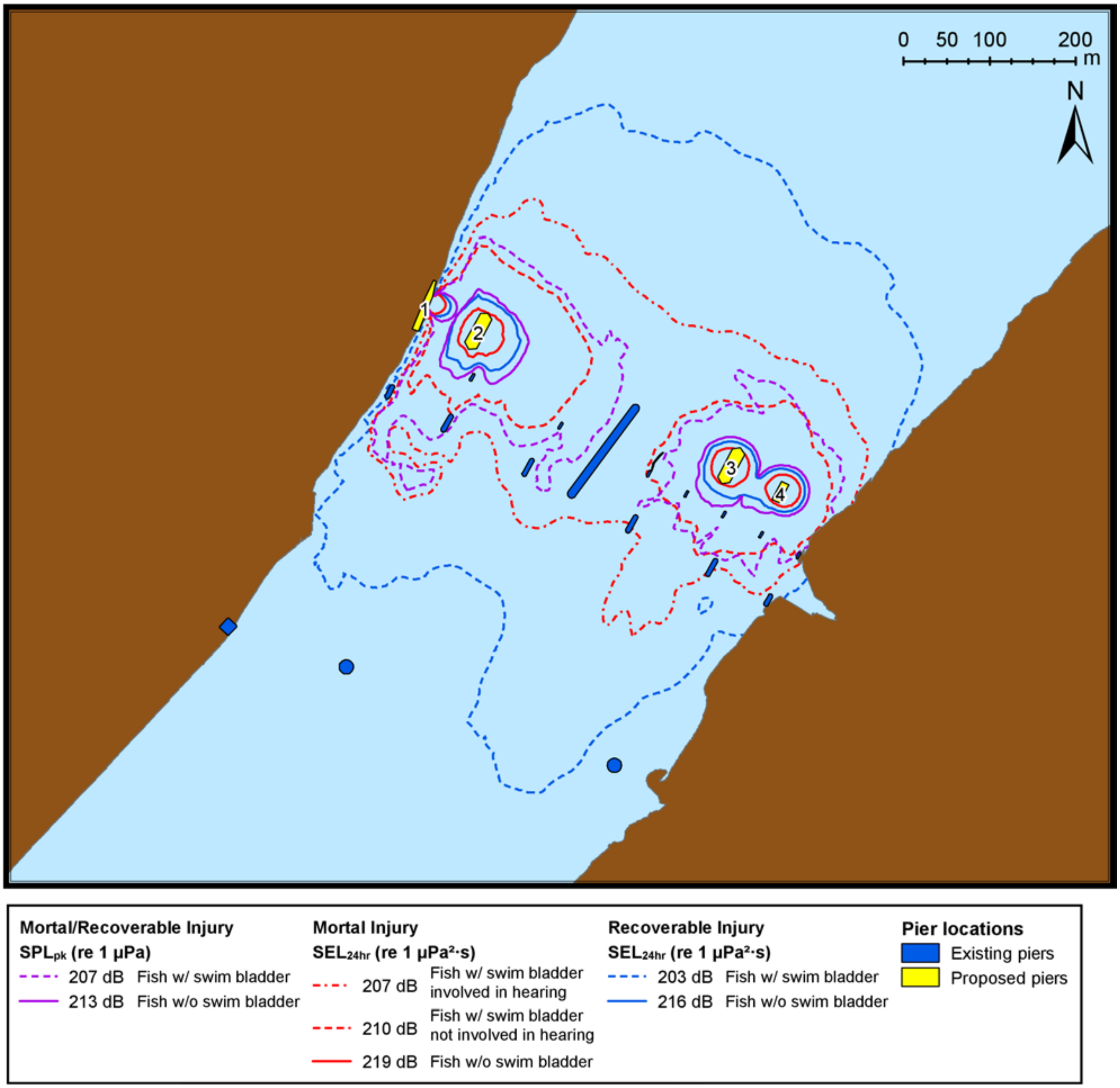

Figure 14. Multi-pile scenario all four sites: Threshold contours based on maximum-over-depth acoustic fields for pile driving using D180-32 impact hammer simultaneously at all four sites.

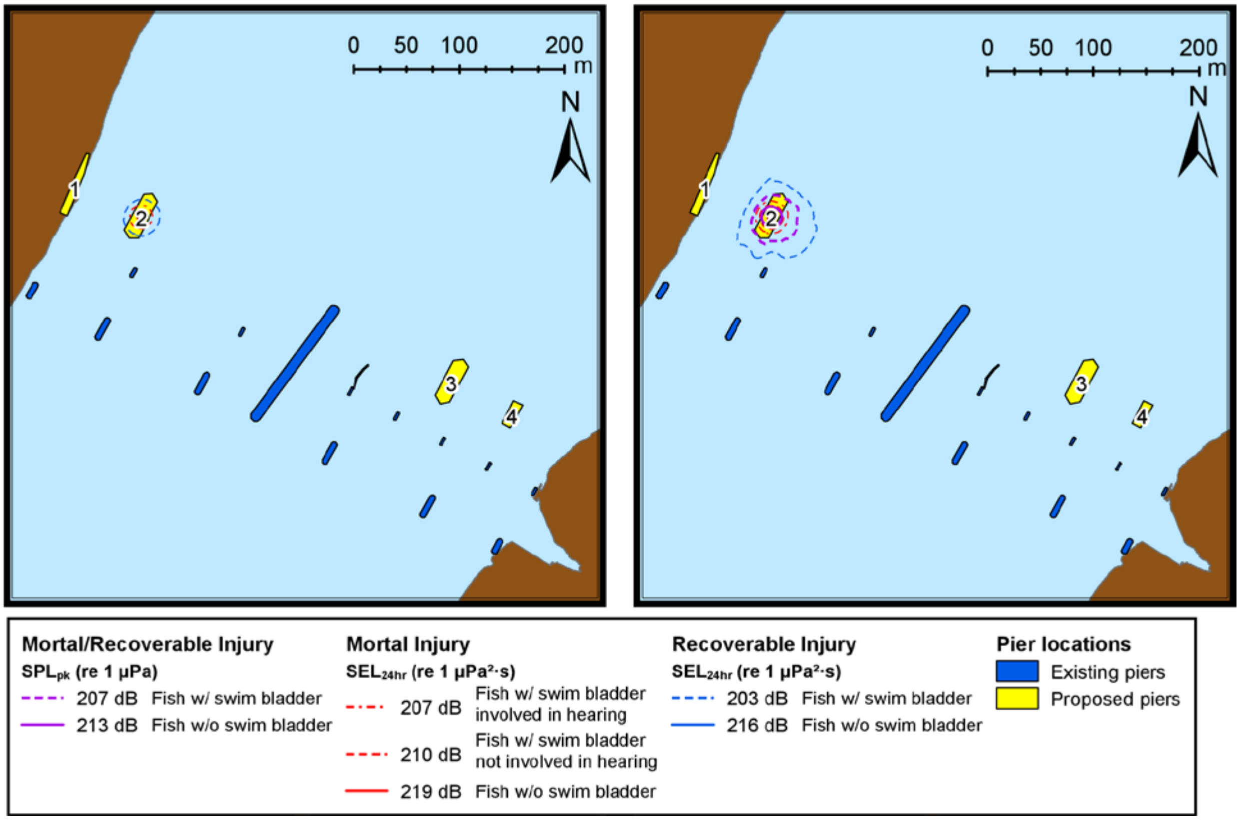

Figure 15. Site 2 (mitigated): Threshold contours based on maximum-over-depth acoustic fields for pile driving using D180-32 impact hammer at Site 2 with mitigation; maximum reduction (left) and minimum reduction (right).

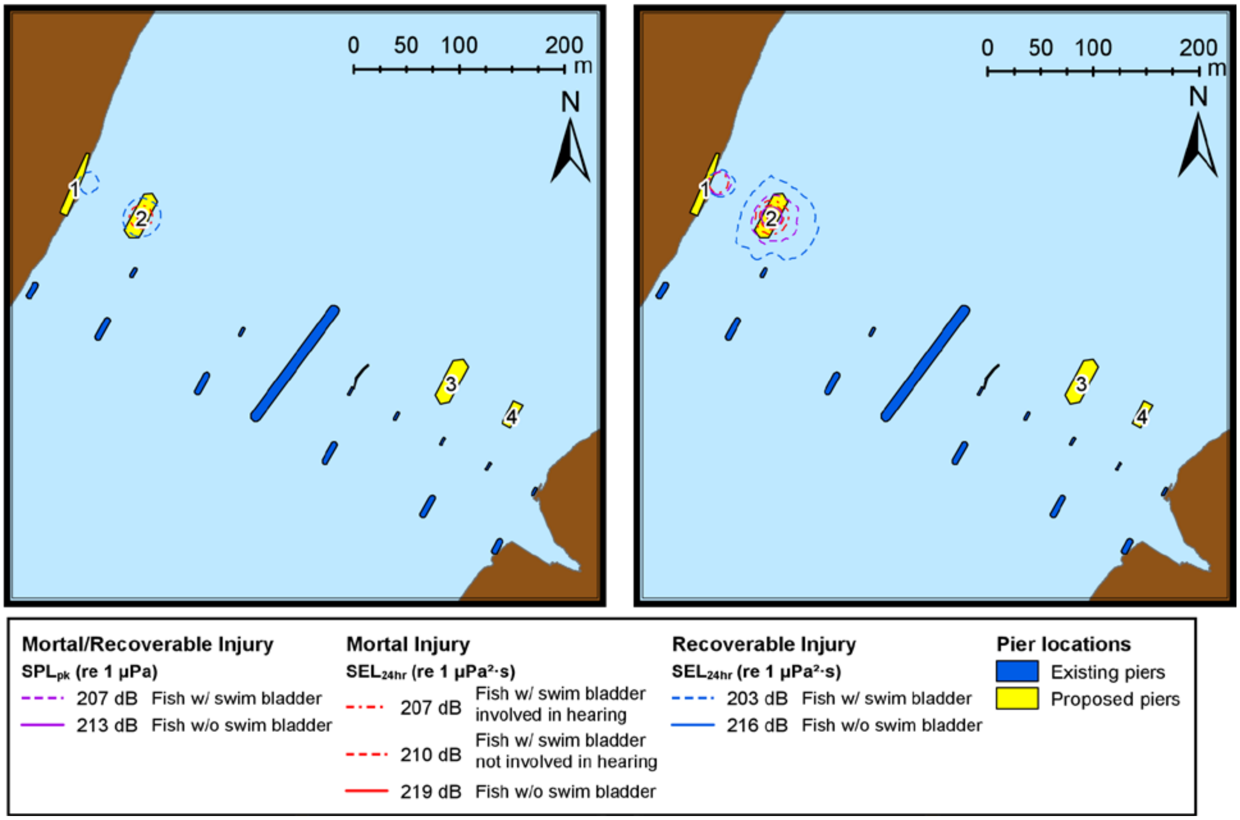

Figure 16. Multi-pile scenario Site 1 + Site 2 (mitigated): Threshold contours based on maximum-over-depth acoustic fields for pile driving using D180-32 impact hammer at Site 1 and 2 simultaneously with mitigation; maximum reduction (left) and minimum reduction (right).

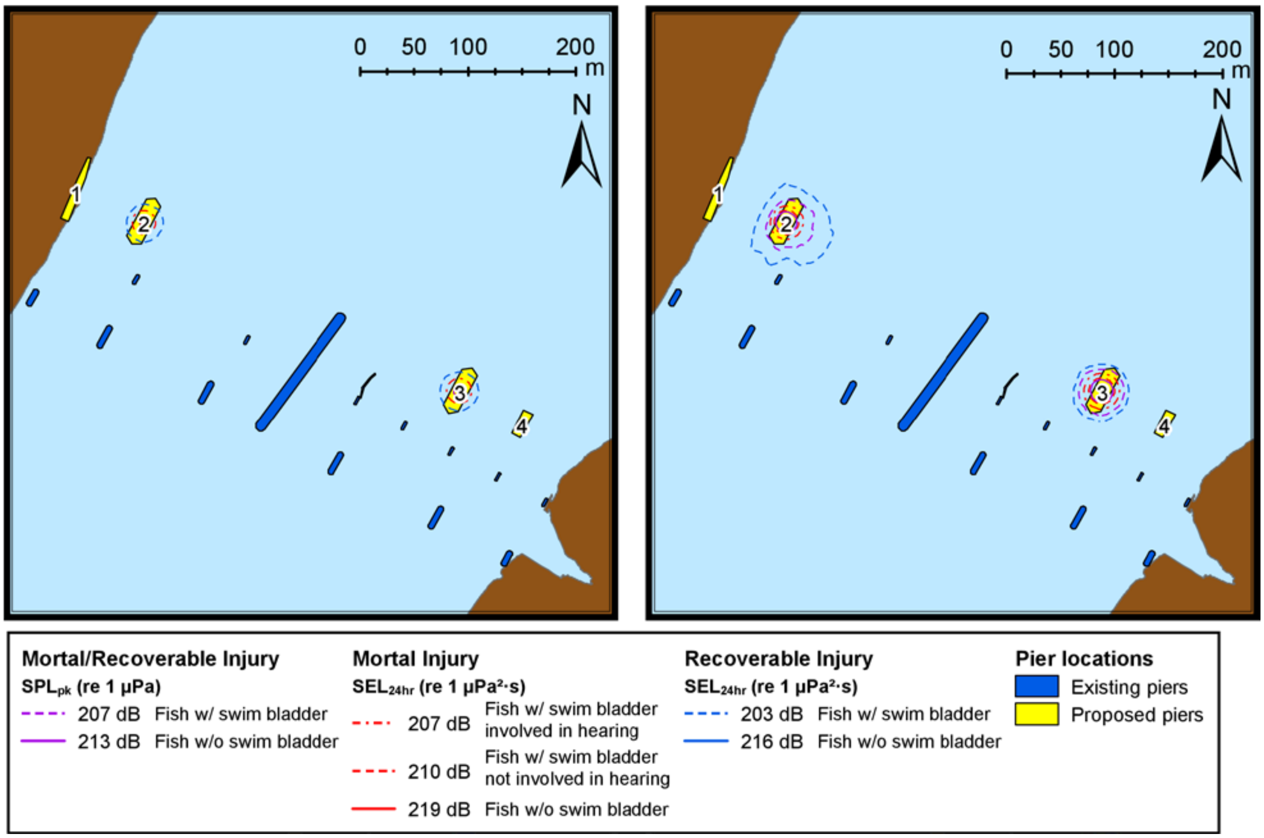

Figure 17. Multi-pile scenario Site 2 + Site 3 (mitigated): Threshold contours based on maximum-over-depth acoustic fields for pile driving using D180-32 impact hammer at Site 2 and 3 simultaneously with mitigation; maximum reduction (left) and minimum reduction (right).

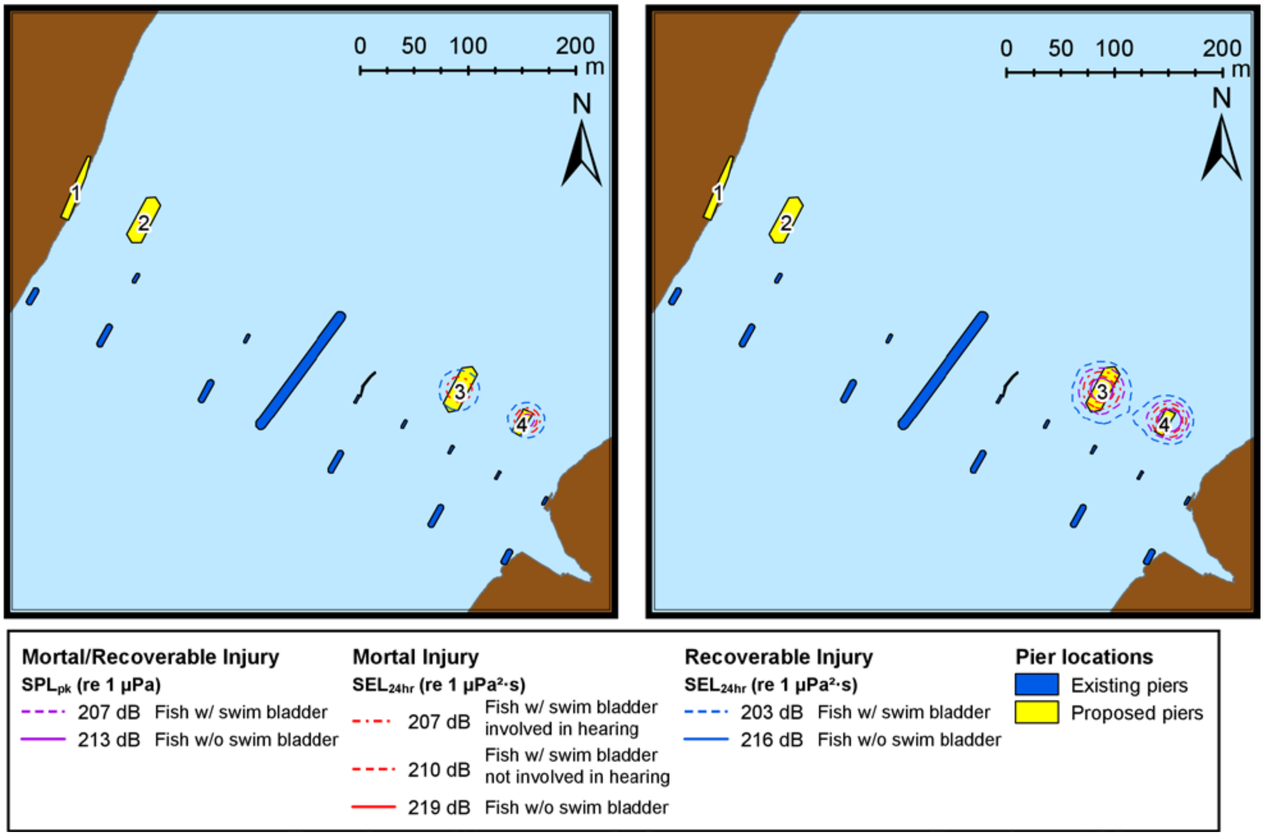

Figure 18. Multi-pile scenario Site 3 + Site 4 (mitigated): Threshold contours based on maximum-over-depth acoustic fields for pile driving using D180-32 impact hammer at Site 3 and 4 simultaneously with mitigation; maximum reduction (left) and minimum reduction (right).

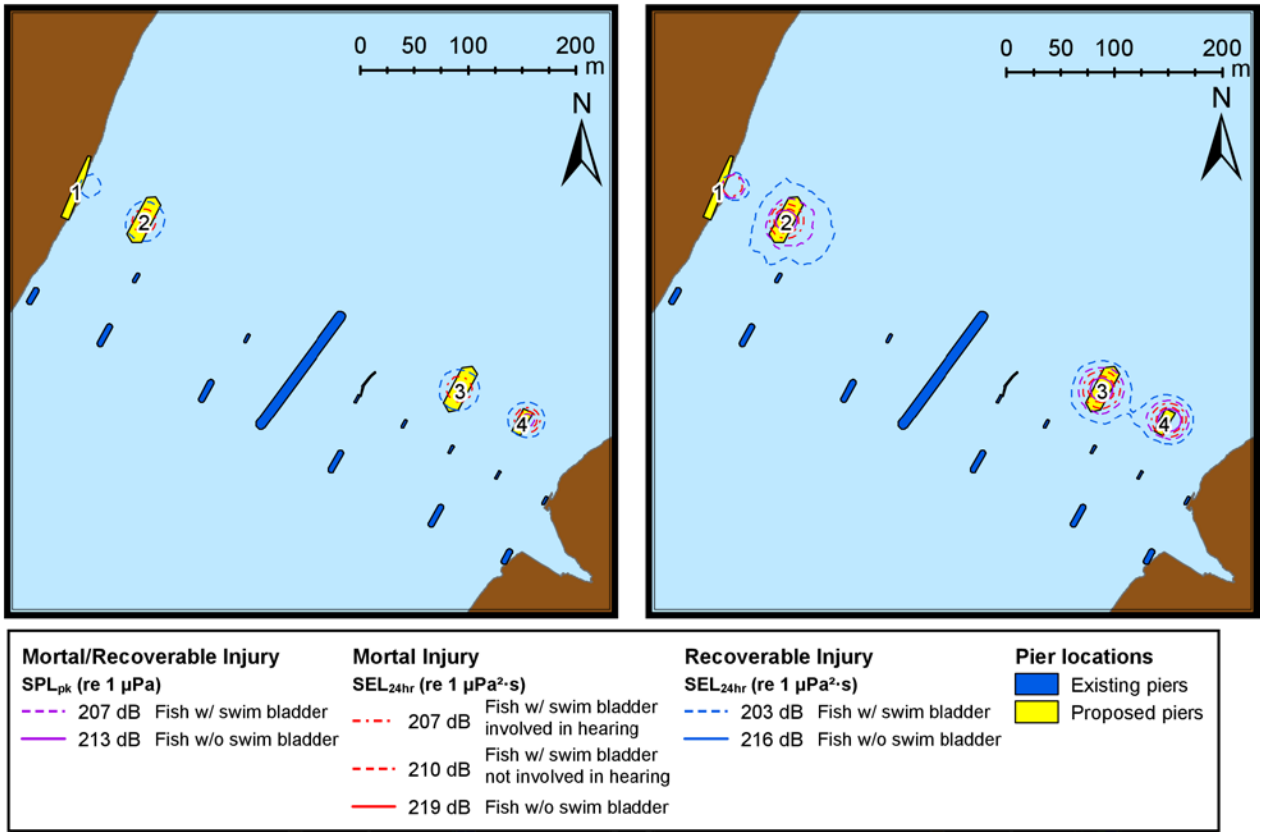

Figure 19. Multi-pile scenario all four sites (mitigated): Threshold contours based on maximum-over-depth acoustic fields for pile driving using D180-32 impact hammer at all four sites simultaneously with mitigation; maximum reduction (left) and minimum reduction (right).

3.3. Sound Field Range

The maximum broadband sound pressure level (SPL) fields for the mitigated multi-pile scenario at all four sites were estimated based on the results of the per-strike SPL modelling. The modelling was performed to the maximum distance of 1 km from the sound source. The graph of variation of maximum per-pulse SPL with distance from the source is provided in Figure 20. The SPL are provided for three cases: no mitigation, minimum mitigation, and maximum mitigation. Using the largest sound mitigation in the Project model, the estimated maximum SPL at 1 km is approximately 163 dB re 1 µPa^{2}·s. Past monitoring studies of sound levels in the Fraser River South arm found that 10 percent of the time, the SPL was higher than 127 dB re 1 µPa, with a median level of 109 dB re 1 µPa and maximum detected level of 136 dB re 1 µPa (BC Ministry of Transportation and Infrastructure 2015).

The Project sound levels exceed the maximum detected ambient (background noise) levels to the edge of the modeling at 1 km from the pile driving operations. Extrapolating from the model, sound levels from the pile driving model attenuate below the maximum ambient levels recorded during the Fraser South arm study at approximately 6 km from the source. However, the extrapolation assumes that a straight line exists between the source and receiver points. Bends in the river and obstructions such as islands located approximately 800 m upstream and 5 km downstream of the proposed construction site, will impact the transmission of sound.

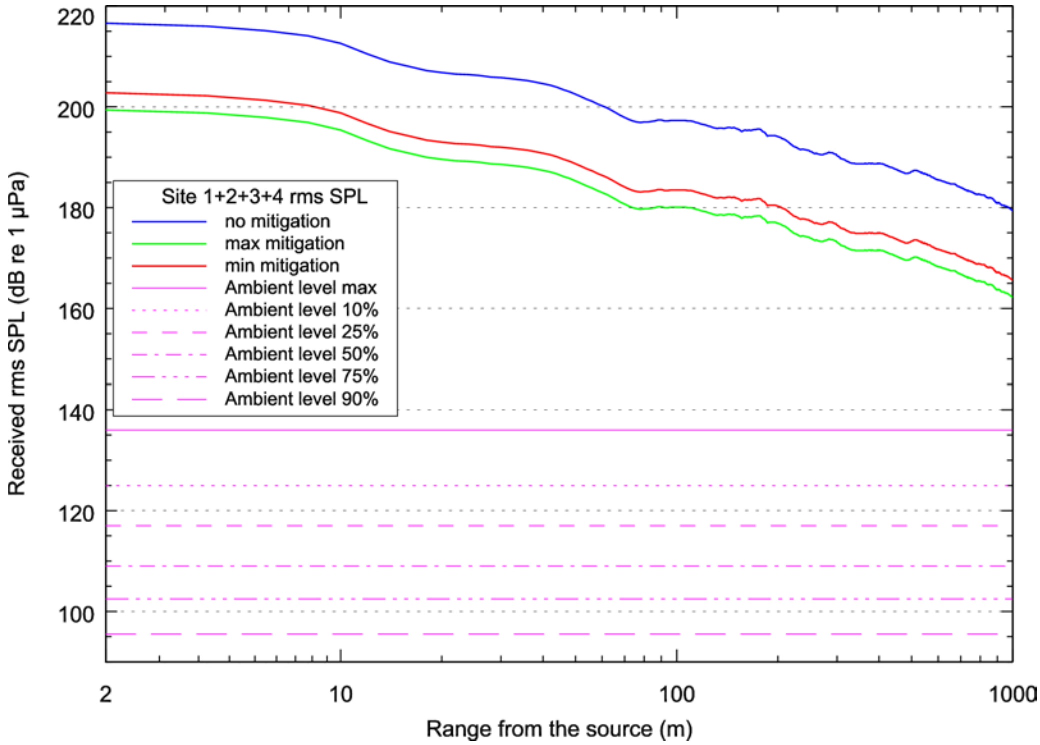

Figure 20. Multi-pile scenario all four sites: variation of the maximum per-strike SPL over distance from the source. The ambient percentile levels are provided after BC Ministry of Transportation and Infrastructure (2015). The percentiles represent the percentage of time the levels were higher than the background noise received levels.

4. Discussion

The effects of sound exposure on fish are less well understood than those on humans or marine mammals. There are significant challenges in not only studying fish responses to sounds, but in extrapolating the results of studies typically conducted in laboratory settings or in open water cages to large numbers of species and variable environments. Even in highly controlled settings, the effects of sound on fish can vary depending on details such as the animal's size and body position relative to the sound source.

Two metrics are considered when assessing the potential injurious effects of sound exposure on fish from impulsive sources such as pile driving. These are SEL, a measure of the time integral of sound energy across multiple exposures (in this case pile strikes over a 24 hour period), which is an index for accumulated sound energy, and L_{pk}, a measure of the maximum absolute value of the instantaneous sound pressure during a specified time interval. Currently there are no international or North American standards for exposure of fish to sound. The criteria used in this analysis from Popper et al. 2014 are considered the best available science for assessing the effects of sound on fish.

The impulsive sounds generated by impact pile driving are characterized by a relatively rapid rise time to a maximal pressure value followed by a decay period that may include a period of diminishing, oscillating maximal and minimal sound pressures (Illingsworth and Rodkin 2001, 2007; Reyff 2012). Tissue damage, or barotrauma, leading to death or injury can result from exposure in both a single strike, and energy accumulated over multiple strikes (SEL). Barotrauma endpoints include lethal injury through immediate mortality or delayed mortality (McKinstry et al. 2007) and a number of injuries with varying severity from which full recovery is possible (e.g., Halvorsen et al. 2011, 2012; Brown et al. 2012; Casper et al. 2012, 2013). Injuries that are potentially recoverable, such as fin haematomas, capillary dilation, and loss of sensory hair cells may still lead to death if they decrease fitness and the animal is subject to predation or disease. Mortality as a result of reduced fitness that leads to predation or disease is classified as indirect mortality, whereas death as a result of injuries is classified as direct mortality (Halvorsen et al. 2011, 2012).

A range of behavioural responses have been observed in studies of wild fish exposed to anthropogenic sound. In these studies, some fishes showed changes in swimming behaviour and orientation, including startle reactions (Pearson et al. 1992; Wardle et al. 2001; Hassel et al. 2004). The response may habituate with repeated presentations of the same sound. Studies conducted in the 1990's (Feist 1992; Anderson 1990) showed that fish might move away from a piling driving source. Wardle et al. (2001) used a video system to examine the behaviours of fish and invertebrates on a coral reef in response to emissions from seismic air guns that were carefully calibrated and measured to have a maximum sound pressure level of 210 dB re 1 µPa at 16 m from the source and 195 dB re 1 µPa at 109 m from the source. They found no permanent changes in the behaviour of the fish or invertebrates on the reef throughout the course of the study, and no animals appeared to leave the reef. There was no indication of any observed damage to the animals (Hastings and Popper 2005).

While few data are available on larval fishes, those species studied appear to have hearing frequency ranges similar to those of adults (Higgs et al. 2002; Egner and Mann 2005; Zeddies and Fay 2005; Wright et al. 2011), and similar acoustic startle thresholds (Zeddies and Fay 2005). Swim bladders may develop during the larval stage and may render larvae susceptible to pressure-related injuries (e.g., barotrauma). The few studies to date on effects on eggs, larvae and fry are insufficient to reach any conclusions with respect to the way sound affects survival (Hastings and Popper 2005). Current concern over the effects of sound on eggs, and especially for larvae containing gas bubbles, is focused on barotrauma rather than hearing.

There are no quantitative criteria for fish behavioural response to sound. The relative risks associated with exposure are presented in Popper et al. 2014 (Table 12).

Table 12. Relative risk of behavioural response for fish at three distances from the pile driving source defined as near (N), intermediate (I) and far (F).

Fish Group	Behaviour
Fish without swim bladder	(N) High, (I) Moderate, (F), Low
Fish with swim bladder not involved in hearing*	(N) High, (I) Moderate, (F), Low
Fish with swim bladder involved in hearing	(N) High, (I) High, (F), Moderate
Eggs and larvae	(N) Moderate, (I) Low, (F), Low

*Notes: SEL_{24hr} = VCs sturgeon and Pacific salmon are fish with swim bladders not involved in hearing

5. Conclusions

The Fraser River is an important transportation route with significant shipping traffic and industrial activity on its banks and islands, including Annacis Island, located South of the proposed Project. Background broadband noise levels recorded in the Fraser River South arm in May 2014, ranged from 94 to 127 dB re 1 µPa, with a median level of 109 dB re 1 µPa. Broadband ambient sound pressure levels exceeded 120 dB re 1 µPa^2, 20 % of the time (BC Ministry of Transportation and Infrastructure 2015). Potential sound levels resulting from the proposed Project pile driving scenarios were modelled using a number of assumptions summarized in Appendix A. Sound exposure levels and sound pressure levels were calculated unmitigated and with mitigation measures applied to reduce sound levels in the water column. Minimum and maximum reduction values from a field test study of a double wall mitigation technique (Reinhall et al. 2015) were used to calculate threshold radii. Applying acoustic thresholds for injury to fish with a swim bladder not involved in hearing from Popper et al. 2014., the modelled range for mortality and potential mortal injury (210 dB SEL and 207 dB SPL) and recoverable injury (203 dB SEL and 207 dB SPL) is limited to a distance very near to the impact pile driving sound source - between 4 and 24 metres ($R_{95\%}$) for all scenarios. These model predictions assume that the biological receiver (e.g., fish) is stationary for the duration of the sound exposure.

Project pile driving sounds are predicted to attenuate to background levels over a distance of several kilometres assuming an unobstructed straight line. River bends, islands and in-river infrastructure will increase the attenuation of sound, therefore modelled ranges to sound levels that could potentially elicit behavioural response are considered conservative.

There are few data to suggest the predicted response of fish, particularly in environments with high sound producing activity levels like the Fraser River. Behavioural response of fish to impulsive sounds including pile driving is highly variable, including no response, startle response, avoidance, and habituation. Fish with swim bladders not involved in hearing, which include sturgeon and Pacific salmon, are predicted to be at moderate risk of behavioural response at intermediate distances (10s of meters from the source) and low risk at greater distances, even when piling source sound levels exceed background noise levels. Eggs and larvae are predicted to be at lower risk than adults for behavioural response.

Literature Cited

ANSI S12.7-1986. R2006. *American National Standard Methods for Measurements of Impulse Noise*. American National Standards Institute, New York.

ANSI S1.1-1994. R2004. *American National Standard Acoustical Terminology*. American National Standards Institute, New York.

BC Ministry of Transportation. 2015. George Massey Tunnel Replacement Project. Part B Underwater Noise Assessment. Prepared by JASCO Applied Sciences for Hemmera.

[DFO] Fisheries and Oceans Canada. 2013. *Fraser River Environmental Watch Report*. http://web.archive.org/web/20140305194012/http://www.pac.dfo-mpo.gc.ca/science/habitat/frw-rfo/reports-rapports/2013/2013-07-02/2013-07-02-eng.html.

[NOAA] National Oceanic and Atmospheric Administration. 2013. *Draft Guidance for Assessing the Effects of Anthropogenic Sound on Marine Mammals: Acoustic Threshold Levels for Onset of Permanent and Temporary Threshold Shifts*. National Oceanic and Atmospheric Administration, U.S. Department of Commerce.

Anderson, J.J. 1990. Assessment of the risk of pile driving to juvenile fish. In: Frauenheim JL (ed) Lessons of the 80's - Strategies of the 90's. Proceedings of the 15th Annual Member's Conference, Deep Foundations Institute, Seattle, Washington, 10–12 October 1990. Deep Foundations Institute, Hawthorne, New Jersey, p 1–11. http://www.cbr.washington.edu/papers/jim/deep.foundations.pdf. Accessed 29 Jan 2013

Betke, K. 2008. *Measurement of Wind Turbine Construction Noise at Horns Rev II.* Report Number 1256-08-a-KB. Report from ITAP–Institut für technische und angewandte Physik GmbH, Oldenburg, Germany, for BioConsultSH, Husun, Germany. 30 pp.

Brown, R.S., Carlson, T.J., Gingerich, A.J. et al. 2012. Quantifying mortal injury of juvenile Chinook salmon exposed to simulated hydro-turbine passage. Trans Am Fish Soc 141(1):147–157. doi: 10.1080/00028487.2011.650274

Buckingham, M.J. 2005. Compressional and shear wave properties of marine sediments: Comparisons between theory and data. *Journal of the Acoustical Society of America* 117(1): 137-152.

Buehler, D., R. Oestman, J. Reyff, K. Pommerenck, and B. Mitchell. 2015. *Technical Guidance for Assessment and Mitigation of the Hydroacoustic Effects of Pile Driving on Fish*. Report Number CTHWANP-RT-15-306.01.01. California Department of Transportation (CALTRANS), Division of Environmental Analysis. 532 pp. http://www.dot.ca.gov/hq/env/bio/files/bio_tech_guidance_hydroacoustic_effects_110215.pdf.

Casper, B.M., Halvorsen, M.B., and A.N. Popper. 2012. Are sharks even bothered by a noisy environment? In: Popper A.N., Hawkins, A.D. (eds). The effects of noise on aquatic life. Springer Science + Business Media, New York, p 93–98

Casper, B.M., Halvorsen, M.B., Matthews, F., Carlson, T.J., and A.N. Popper. 2013. Recovery of barotrauma injuries resulting from exposure to pile driving sounds in two sizes of hybrid striped bass. PLoS ONE 8(9):e73844. doi:10.1371/journal.pone.0073844

Feist, B.E. 1992. Potential impacts of pile driving on juvenile pink (*Oncorhyncus gorbuscha*) and chub (*O. keta*) salmon behavior and distribution. MS Thesis, University of Washington

Halvorsen, M.B., Casper, B.M., Woodley, C.M., Carlson, T.J. and A.N. Popper. 2011. Predicting and mitigating hydroacoustic impacts on fish from pile installations. NCHRP Res Results Digest 363 Project 25–28, National Cooperative Highway Research Program, Transportation Research Board, National Academy of Sciences, Washington, D.C. http://www.trb.org/Publications/Blurbs/166159.aspx.

Hassel, A., Knutsen T., Dalen, J. et al. 2004. Influence of seismic shooting on the lesser sand eel (*Ammodytes marinus*). J Marine Sci 61:1165–1173

Hastings, M.C. and A.N. Popper. 2005. *Effects of Sound on Fish*. Volume Prepared by Jones & Stokes under California Department of Transportation Contract No. 43A0139, Task Order 1, Sacramento, CA. 82 pp.

Higgs, D.M., Souza M.J., Wilkins H.R., Presson J.C. and A.N. Popper (2002) Age- and size-related changes in the inner ear and hearing ability of the adult zebrafish (*Danio rerio*). J Assn Res Otolaryngol 3:174–184

Illingsworth, R. and R. Rodkin. 2001. Noise and vibration measurements associated with the pile installation demonstration project for the San Francisco-Oakland Bay Bridge east span. Technical Report of Illingsworth & Rodkin, Inc. Petaluma, CA

Illingsworth, R. and R. Rodkin. 2007. Compendium of pile driving sound data. Prepared for the California Department of Transportation, Sacramento, CA, September 27, 2007

Lippert, S., M. Nijhof, T. Lippert, D. Wilkes, A. Gavrilov, K. Heitmann, M. Ruhnau, O. von Estorff, A. Schäfke, et al. 2016. COMPILE—A Generic Benchmark Case for Predictions of Marine Pile-Driving Noise. *IEEE Journal of Oceanic Engineering* 41(4): 1061-1071. 10.1109/JOE.2016.2524738.

MacGillivray, A. 2014. A model for underwater sound levels generated by marine impact pile driving. *Proceedings of Meetings on Acoustics* 20(1): 045008. http://scitation.aip.org/content/asa/journal/poma/20/1/10.1121/2.0000030.

MacGillivray, A.O. and N.R. Chapman. 2012. Modeling underwater sound propagation from an airgun array using the parabolic equation method. *Canadian Acoustics* 40(1): 19-25. http://jcaa.caa-aca.ca/index.php/jcaa/article/view/2502.

Mann, D.A., A.N. Popper, and B. Wilson. 2005. Pacific herring hearing does not include ultrasound. *Biology Letters* 1(2): 158-161.

Marczak, W. 1997. Water as a standard in the measurements of speed in sound in liquids. *Journal of the Acoustical Society of America*: 2776-2779.

McKinstry, C., Carlson, T., and R. Brown. 2007. Derivation of a mortal injury metric for studies of rapid decompression of depth-acclimated physostomous fish. PNNL-17080, Pacific Northwest National Laboratory, Richland, WA. http://www.pnl.gov/main/publications/external/technical_reports/PNNL-17080.pdf. Accessed 20 Dec 2013

Pearson, W.H., J.R. Skalski, and C.I. Malme. 1992. Effects of sounds from a geophysical survey device on behavior of captive rockfish (Sebastes spp.). *Canadian Journal of Fisheries and Aquatic Sciences* 49(7): 1343-1356. http://www.nrcresearchpress.com/doi/abs/10.1139/f92-150.

Pile Dynamics, Inc. 2010. GRLWEAP.

Popper, A.N., A.D. Hawkins, R.R. Fay, D.A. Mann, S. Bartol, T.J. Carlson, S. Coombs, W.T. Ellison, R.L. Gentry, et al. 2014. *Sound Exposure Guidelines for Fishes and Sea Turtles: A Technical Report prepared by ANSI-Accredited Standards Committee S3/SC1 and registered with ANSI*. SpringerBriefs in Oceanography, Volume ASA S3/SC1.4 TR-2014. ASA Press.

Reyff, J.A. 2012. Underwater sounds from unattenuated and attenuated marine pile driving. In Popper AN, Hawkins AD (eds) The effects of noise on aquatic life. Springer Science + Business Media, LLC New York, p 439–444

Wardle, C.S., Carter, T.J., Urquhart, G.G. et al. 2001. Effects of seismic airguns on marine fish. Cont Shelf Res 21: 1005–1027.

Wright, K.J., Higgs D.M. and J.M. Leis. 2011. Ontogenetic and interspecific variation in hearing ability in marine fish larvae. Mar Ecol Prog Ser 424:1–13

Zeddies, D.G. and R.R. Fay. 2005. Development of the acoustically evoked behavioral response in zebrafish to pure tones. *Journal of Experimental Biology* 208(7): 1363-1372. http://jeb.biologists.org/content/208/7/1363.long.

Appendix A. Summary of Study Assumptions

A summary of the assumptions used in this study, including inputs and the methods used for modelling are presented in Table A-1.

Table A-1. Summary of model inputs, assumptions, and methods.

Parameter	Description
Pile Driving Source Model	
Modelling method	Finite-difference structural model of pile vibration based on thin-shell theory; hammer forcing functions computed using GRLWEAP
Impact hammer model	Delmag D180-32
Impact hammer energy	600 kJ
Ram weight	176.6 kN
Helmet weight (20% of ram weight)	35.3 kN
Strike rate	30
Estimated number of strikes to drive pile	700
Modelled number of strikes per pile	1000
Number of piles per site per day	1
Pile length	50 m in-sediment + 8 m above water + water depth
Pile diameter	180 cm
Modelled seabed penetration	50 m
Cumulative SEL calculation	Per-pulse sound exposures assumed to be equal over duration of drive
Environmental Parameters	
Sound Speed Profile	Constant speed based on mean temperature for spring-summer season
Bathymetry	Contour lines 0.5 m step based on data collected in 2011 and 2014
Geoacoustics	Elastic seabed properties based on client-supplied surficial sediment samples description.
Propagation model	
Modelling method	FWRAM full-waveform parabolic-equation propagation model; single transect
Source representation	Vertical line array
Separation between discrete sources representing pile	0.37 m
Virtual receiver depths	1-26 m with 1 m step
Frequency range	10-2048 Hz
Synthetic trace length	500 ms
Maximum modelled range	1 km

Appendix B. Glossary

1/3-octave-band
Non-overlapping passbands that are one-third of an octave wide (where an octave is a doubling of frequency). Three adjacent 1/3-octave-bands make up one octave. One-third-octave-bands become wider with increasing frequency. See also octave.

absorption
The conversion of acoustic energy into heat.

attenuation
The gradual loss of acoustic energy from absorption and scattering as sound propagates through a medium.

azimuth
A horizontal angle relative to a reference direction, which is often magnetic north or the direction of travel. In navigation, it is also called bearing.

bandwidth
The range of frequencies over which the context refers, e.g., acoustic signature or recording.

broadband sound level
The total sound pressure level measured over a specified frequency range. If the frequency range is unspecified, it refers to the entire measured frequency range.

compressional wave
A mechanical vibration wave in which the direction of particle motion is parallel to the direction of propagation. Also called primary wave or P-wave.

decibel (dB)
One-tenth of a bel. Unit of level when the base of the logarithm is the tenth root of ten, and the quantities concerned are proportional to power (ANSI S1.1-1994 R2004).

frequency
The rate of oscillation of a periodic function measured in cycles-per-unit-time. The reciprocal of the period. Unit: hertz (Hz). Symbol: f. 1 Hz is equal to 1 cycle per second.

geoacoustic
Relating to the acoustic properties of the seabed.

hertz (Hz)
A unit of frequency defined as one cycle per second.

impulsive sound
Sound that is typically brief and intermittent with rapid (within a few seconds) rise time and decay back to ambient levels (NOAA and US Dept of Commerce 2013, ANSI S12.7-1986 R2006). For example, seismic airguns and impact pile driving.

octave
The interval between a sound and another sound with double or half the frequency. For example, one octave above 200 Hz is 400 Hz, and one octave below 200 Hz is 100 Hz.

parabolic equation method
A computationally-efficient solution to the acoustic wave equation that is used to model transmission loss. The parabolic equation approximation omits effects of back-scattered sound, simplifying the computation of transmission loss. The effect of back-scattered sound is negligible for most ocean-acoustic propagation problems.

peak sound pressure level (peak SPL)
The maximum instantaneous sound pressure level, in a stated frequency band, within a stated period. Also called zero-to-peak sound pressure level. Unit: decibel (dB).

point source
A source that radiates sound as if from a single point (ANSI S1.1-1994 R2004).

pressure, acoustic
The deviation from the ambient hydrostatic pressure caused by a sound wave. Also called overpressure. Unit: pascal (Pa). Symbol: p.

pressure, hydrostatic
The pressure at any given depth in a static liquid that is the result of the weight of the liquid acting on a unit area at that depth, plus any pressure acting on the surface of the liquid. Unit: pascal (Pa).

propagation loss
The decibel reduction in sound level between two stated points that results from sound spreading away from an acoustic source subject to the influence of the surrounding environment. Also called transmission loss.

received level
The sound level measured at a receiver.

rms
root-mean-square.

rms sound pressure level (rms SPL)
The root-mean-square average of the instantaneous sound pressure as measured over some specified time interval. For continuous sound, the time interval is one second. See also sound pressure level (SPL) and 90% rms SPL.

shear wave
A mechanical vibration wave in which the direction of particle motion is perpendicular to the direction of propagation. Also called secondary wave or S-wave. Shear waves propagate only in solid media, such as sediments or rock. Shear waves in the seabed can be converted to compressional waves in water at the water-seabed interface.

sound exposure
Time integral of squared, instantaneous frequency-weighted sound pressure over a stated time interval or event. Unit: pascal-squared second (Pa2·s) (ANSI S1.1-1994 R2004).

sound exposure level (SEL)
A measure related to the sound energy in one or more pulses. Unit: dB re 1 µPa2·s.

sound field
Region containing sound waves (ANSI S1.1-1994 R2004).

sound pressure level (SPL)
The decibel ratio of the time-mean-square sound pressure, in a stated frequency band, to the square of the reference sound pressure (ANSI S1.1-1994 R2004).

For sound in water, the reference sound pressure is one micropascal (p0 = 1 µPa) and the unit for SPL is dB re 1 µPa:

$$SPL = 10\log_{10}\left(p^2 / p_0^2\right) = 20\log_{10}\left(p / p_0\right)$$

Unless otherwise stated, SPL refers to the root-mean-square sound pressure level (rms SPL).

sound speed profile
The speed of sound in the water column as a function of depth below the water surface.

source level (SL)
The sound pressure level measured 1 metre from a theoretical point source that radiates the same total sound power as the actual source. Unit: dB re 1 µPa @ 1 m

Appendix C. Sound Metrics Used in Pile Modelling

Underwater sound amplitude is measured in decibels (dB) relative to a fixed reference pressure of p_o = 1 μPa. Because the loudness of impulsive (pulsed) sounds, e.g., shots from seismic source arrays, is not generally proportional to the instantaneous acoustic pressure, several sound level metrics are commonly used to evaluate the loudness of impulsive sound and its effects on marine life.

The zero-to-peak sound pressure level (SPL), or peak SPL (L_{pk}, dB re 1 μPa), is the maximum instantaneous sound pressure level in a stated frequency band attained by an impulse, $p(t)$:

$$L_{\mathrm{pk}} = 10\log_{10}\left[\frac{\max\left(\left|p^2(t)\right|\right)}{p_{\mathrm{o}}^2}\right] \quad \text{(C-1)}$$

The sound exposure level (SEL) (L_E, dB re 1 μPa²·s) is the time integral of the squared pressure in a stated frequency band over a stated time interval or event. The per-pulse SEL is calculated over the time window containing the entire pulse (i.e., 100% of the acoustic energy), T_{100}:

$$L_E = 10\log_{10}\left(\int_{T_{100}} p^2(t)dt \Big/ T_{\mathrm{o}} p_{\mathrm{o}}^2\right) \quad \text{(C-2)}$$

where T_o is a reference time interval of 1 s. The per-pulse SEL, with units of dB re 1 μPa·√s, or equivalently dB re 1 μPa²·s, represents the total acoustic energy delivered over the duration of the acoustic event at a receiver location. It is a measure of sound energy (or exposure) rather than sound pressure although it is not measured in energy units.

SEL is a cumulative metric that is calculated over a specified time period that may contain multiple pulses. SEL can be computed by summing (in linear units) the SELs of the N individual pulses (L_{Ei}).

$$L_{E\mathrm{c}} = 10\log_{10}\left(\sum_{i=1}^{N} 10^{\frac{L_{Ei}}{10}}\right) \quad \text{(C-3)}$$